Structure and flow behaviour of block copolymers

2001 J. Phys.: Condens. Matter 13 R643

(http://iopscience.iop.org/0953-8984/13/33/201)

INSTITUTE OF PHYSICS PUBLISHING JOURNAL OF PHYSICS: CONDENSED MATTER

J. Phys.: Condens. Matter **13** (2001) R643–R671 PII: S0953-8984(01)18015-X

REVIEW ARTICLE

Structure and flow behaviour of block copolymers

Ian W Hamley

School of Chemistry, University of Leeds, Leeds LS2 9JT, UK

Received 25 June 2001
Published 2 August 2001
Online at stacks.iop.org/JPhysCM/13/R643

Abstract

This review focuses on the effect of flow fields on the orientation of block copolymer nanostructures in the melt and in solution. In particular, the alignment induced by strong shear fields or large extensional flows applied to model diblock and triblock copolymers is considered. The distinct orientation states of lamellar, hexagonal-packed cylinder, cubic micellar and bicontinuous cubic structures under different deformation conditions are summarized and the mechanisms of orientation are discussed.

1. Introduction

Block copolymer melts and solutions are fascinating complex fluids because they can self-assemble into a wide range of nanoscale structures, which can be functionalized for a wide range of potential applications in fields as diverse as optoelectronics, sensing, filtration and catalysis.

The phase behaviour of block copolymer melts is, to a first approximation, represented in a morphology diagram in terms of χN and f [1]. Here f is the volume fraction of one block, and χ is the Flory–Huggins interaction parameter (inversely proportional to temperature) that reflects the interaction energy between different segments. The configurational entropy contribution to the Gibbs energy is proportional to N, the degree of polymerization. When the product χN exceeds a critical value, $(\chi N)_{ODT}$ (ODT = order–disorder transition) the block copolymer microphase separates into a periodically ordered structure, with a lengthscale ∼5–500 nm. The structure that is formed depends on the copolymer architecture and composition [1]. For diblock copolymers, a lamellar (lam) phase is observed for symmetric diblocks ($f = 0.5$), whereas more asymmetric diblocks form hexagonal-packed cylinder (hex) or body-centred cubic (bcc) spherical structures. A complex bicontinuous cubic gyroid (gyr) (spacegroup $Ia\bar{3}d$) phase has also been identified [2, 3] for block copolymers between the lam and hex phases near the ODT, and a hexagonal-perforated layer (HPL) phase has been found to be metastable in this region [4–6]. For ABC triblocks, the introduction of a third component leads to a dramatic increase in the number of possible microstructures [7], only a few of which have so far been observed. Summaries of work on ABC triblock morphologies have appeared [1, 8]. Because of the large number of possible morphologies, theorists are presently working

to predict the phase behaviour of these copolymers using methods that do not require *a priori* knowledge of the space group symmetries of trial structures [9, 10].

To establish the relationships between different block copolymer phase diagrams and also to facilitate comparison with theory, it is necessary to specify parameters in addition to χN and f. First, asymmetry of the conformation of the copolymer breaks the symmetry of the phase diagram about $f = 0.5$. For AB diblocks, conformational asymmetry is quantified using the 'asymmetry parameter' $\varepsilon = (b_A^2/v_A)/(b_B^2/v_B)$ [11, 12], where b_J is the segment length for block J and v_J is the segment volume. Composition fluctuations also modify the phase diagram and this has been accounted for theoretically via the Ginzburg parameter $\bar{N} = Nb^6\rho^2$, where ρ is the number density of chains [13, 14].

A phase diagram computed using self-consistent mean field theory [15, 16] is shown in figure 1. This shows the generic sequence of phases accessed just below the ODT temperature for diblock copolymers of different compositions. The features of the phase diagrams for particular systems are different in detail, but qualitatively they are similar, and well accounted for by self-consistent field theory, which is one of the most successful semi-quantitative theories for the thermodynamic and structural properties of any soft material.

In a solvent, block copolymer phase behaviour is controlled by the interaction between the segments of the polymers and the solvent molecules as well as the interaction between the two blocks. If the solvent is unfavourable for one block this can lead to micelle formation in dilute solution. The phase behaviour of concentrated solutions can be mapped onto that of block copolymer melts [17]. Lamellar, hexagonal-packed cylinder, micellar cubic and bicontinuous cubic structures have all been observed. These are all lyotropic liquid crystal phases, similar to those observed for non-ionic surfactants.

In this review the focus is on the correlation between the structure and flow behaviour of block copolymer melts and solutions. Strong flow fields lead to the macroscopic orientation of microphase-separated structures. In turn, the rheological behaviour of aligned samples depends on the extent of alignment so there is an intimate coupling between the dynamic, mechanical and thermodynamical properties. The first studies of flow-induced orientation in block copolymers were for commercial thermoplastic elastomers subjected to extensional flow in extrusion [18–20]. This illustrates the relevance of fundamental research on correlations between flow behaviour and structure to the processing of this industrially important class of polymer.

Several reviews on the effect of shear on block copolymers have recently appeared. The influence of shear on block copolymer melts has been considered by Fredrickson and Bates [21], Ryan and Hamley [8] and Hamley [1]. Work using other deformation methods (extension, compression) as well as shear fields to orient block copolymers has been summarized by Honeker and Thomas [22]. The effect of shear on block copolymer solutions has been reviewed by Watanabe [23] and Hamley [1, 24, 25].

2. Lamellar phase

The lam phase is the most widely studied of block copolymer morphologies. It is now well established that long-range order of alternating layers can be induced by the application of large amplitude oscillatory shear (LAOS). Early work on orientation in lamellar block copolymers was undertaken by Keller and coworkers using extrusion techniques [26, 27], which is relevant to processing. However, shear fields are easier to characterize and thus have been employed for most fundamental research.

The effect of LAOS on the ordering of lamellar diblock copolymer melts has been reviewed [28]. Large amplitude shear can be used to change the orientation of the lam phase. The

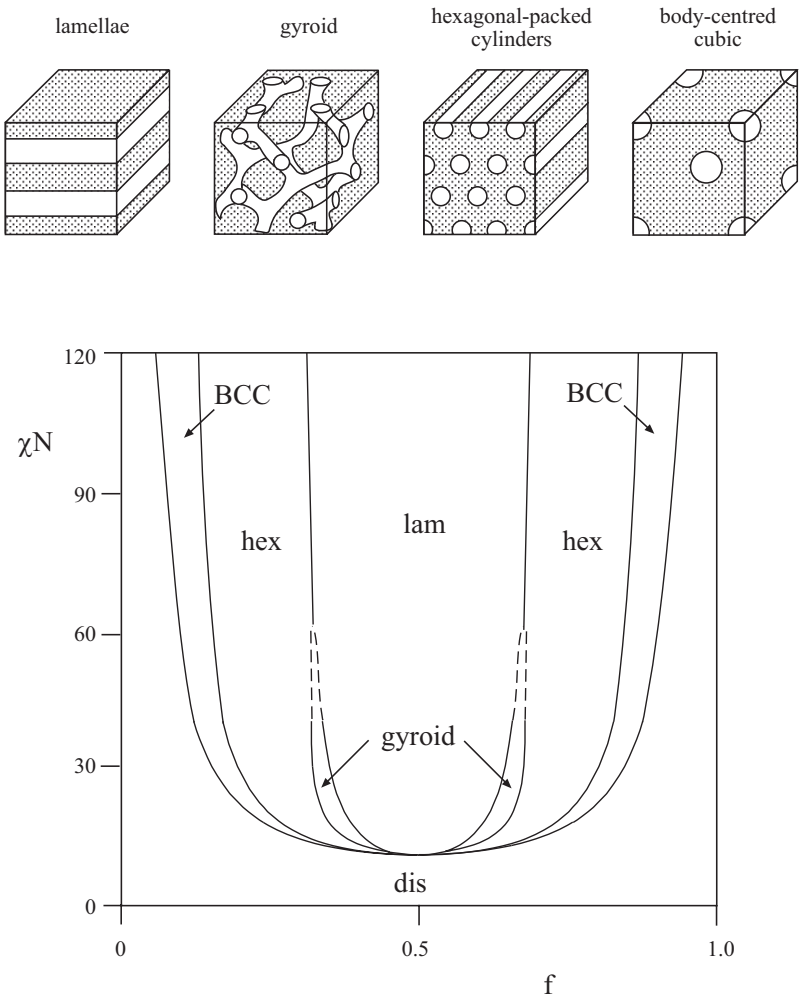

Figure 1. Phase diagram for a conformationally symmetric diblock copolymer, calculated using self-consistent mean field theory [15, 16], along with illustrations of the equilibrium morphologies. In the phase diagram, regions of stability of disordered (dis), lamellar (lam), gyroid (gyr), hexagonal (hex), body-centred cubic (bcc) phases are indicated.

first such observation was made by Koppi *et al* [29] who found, using small-angle neutron scattering (SANS), that two orientations could be accessed in a poly(ethylene-propylene)–poly(ethylethylene) (PEP–PEE) diblock subjected to $\lambda = 100\%$ dynamic shear (where λ is the strain amplitude) depending on the shear rate and temperature. A perpendicular orientation was obtained at high frequencies and high temperatures, the so-called parallel orientation being obtained otherwise. In the parallel orientation the layers align with their normals along the gradient direction, $\nabla \boldsymbol{v}$, whereas in the perpendicular orientation the layer normals lie along the neutral direction, $\boldsymbol{e}$ (figure 2). The transverse orientation (layer normals along the shear direction, $\boldsymbol{v}$) has also been observed, although usually as a transient non-equilibrium state (figure 2).

Koppi *et al* found that the perpendicular orientation could be obtained by shearing a sample

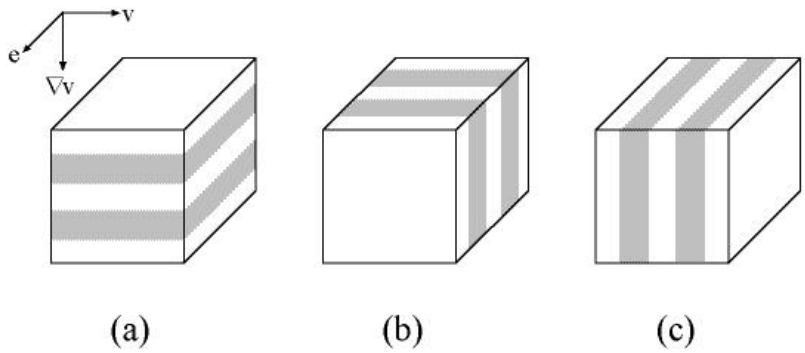

Figure 2. Orientations of a lamellar structure with respect to the shear plane ($\boldsymbol{v}$, $\boldsymbol{e}$): (a) parallel, (b) perpendicular and (c) transverse.

in the parallel orientation at a higher shear rate. However, the reverse process (perpendicular–parallel) was not observed. The high-frequency behaviour near the ODT was interpreted as the result of shear-induced disordering, followed by reordering in the perpendicular orientation. The parallel orientation was believed to result from defect-mediated growth [29].

The transverse orientation that is not found for low molecular weight diblocks was observed for poly(styrene)–poly(isoprene) (PS–PI) diblocks of intermediate molecular weight by Zhang and Wiesner [30]. They deduced this orientation from small-angle x-ray scattering (SAXS) experiments on samples presheared at high frequency and interpreted it in terms of topological constraints due to entanglements of PI. This was also noted by Fredrickson and Bates [21] who pointed out that the mechanical contrast of PS–PI (PS unentangled, PI entangled) is distinct from that for a mechanically balanced system where both components are well above their glass transition temperature. The proximity of the glass transition in PS to the ODT in PS–PI samples also means that the mechanical contrast in systems containing PS can be highly temperature sensitive. A parallel orientation has been observed at high frequency and/or low temperature and a perpendicular orientation at low frequency and/or low temperature for PS–PI diblocks [31, 32]. Zhang *et al* [33] provide a unified picture for low molecular weight PS–PI polymers, with changes in lamellar orientation as a function of reduced frequency (figure 3). At high frequencies, they suggest that the observed parallel orientation arises from mechanical contrast between PS and PI blocks. At intermediate frequencies, lamellar interface destruction and reorganization occurs leading to a perpendicular orientation whilst at low frequencies the interface reorients as a whole leading to a parallel orientation again [33].

The evolution of microstructural orientation in block copolymers was studied in real time by Kornfield and coworkers using birefringence measurements on diblocks sheared *in situ* [34, 35]. The birefringence of the polymer in two orthogonal planes was measured using laser light incident along the vorticity direction or velocity gradient direction in a planar shear geometry, and this could be directly correlated to changes in the dynamic mechanical properties. There are two contributions to the birefringence of an ordered block copolymer. The intrinsic birefringence is due to the tendency of chains to segregate away from microdomain interfaces and the form birefringence is due to the anisotropy of the microphase separated structure. Both contributions are coaxial under weak flow conditions so that the principal axes of the refractive index tensor correspond to those of the ordered structure (e.g. the lamellar normal $\boldsymbol{n}$). The birefringence observed in PEP–PEE diblocks is primarily intrinsic, whereas PS–PI

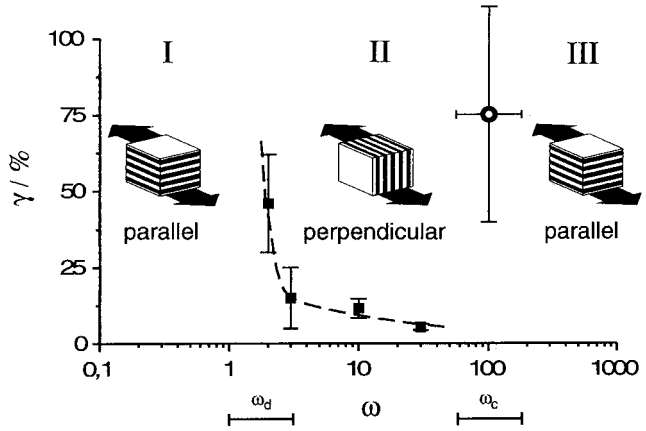

Figure 3. Orientation diagram (strain *versus* shear frequency) for the lam phase of PS–PI diblock copolymers under LAOS in the vicinity of the order–disorder transition [129]. A slice through the three-dimensional orientation diagram (including temperature as the third axis) for a nearly symmetric PS–PI diblock is depicted at $T = 409$ K. The characteristic frequencies separating the three regimes at higher strain values are denoted ω_d at low frequency and ω_c at high frequency. Filled symbols indicate the positions of a transition from parallel-to-perpendicular orientation on increasing strain. The dotted line through these points is a guide for the eye. The open symbol indicates the flipping point from perpendicular-to-parallel orientations at higher strain values, as observed by Gupta *et al* [130].

copolymers possess predominantly form birefringence [21]. For the PEP–PEE diblock studied by Koppi *et al* [29], Kannan and Kornfield [34] observed that the flow process leading to the parallel alignment was associated with inhomogeneous deformation, such that the ordered domains in the polymer were rocked irreversibly into alignment. In contrast, the process that produced perpendicular orientation occurred under conditions in which the deformation was nearly homogeneous. Later, the evolution of orientation in a nearly symmetric PS–PI diblock was studied using the same technique [35]. It was found that at high frequencies a parallel alignment was obtained, whereas at lower frequencies the perpendicular orientation resulted, in contrast to the results on the PEP–PEE diblock [29]. In either case, the alignment process was observed to proceed via an initial fast process, followed by a slow one ($\sim$1 h) [35]. The fast process was dominated by depletion of lamellae in the transverse ('forbidden') orientation when forming the ultimate perpendicular orientation and depletion of perpendicular lamellae when developing the ultimate parallel lamellar structure. In both cases, enhancement of the orientation distribution towards the ultimate alignment was noted. The resulting biaxial distributions were transformed into a uniaxial one during the slow process. During the slow process, the viscoelastic properties were not observed to change significantly [35]. A biaxial lamellar structure has been observed using SAXS on a sheared poly(styrene)–poly(ethylene-propylene) (PS–PEP) diblock [36], and in a PS–PI diblock [30].

Polis and Winey [37] used transmission electron microscopy (TEM) to investigate a biaxial morphology in a sheared PS–PEP (Kraton^{TM}) sample, where kink bands were observed between parallel and transverse lamellae. An example of a kink band is illustrated in figure 4. The formation of kink bands suggested that the transverse lamellae could be the result of buckling of perpendicular lamellae. Relaxation of the kink band structure during quiescent annealing occurred through lamellar tilting rather than twisting, leading to a variety of defect structures [37]. Later they showed that steady shear can be used to induce kink bands, above

a critical shear strain [38]. They performed transmission electron microscopy (TEM) and SAXS experiments on the same diblock. The formation of kink bands was explained by the rotation of lamellae. Based on this mechanism, together with the characteristic size of the kink bands and their spatial distribution, they suggested that kink bands were initiated by pre-existing defects. These results also suggested a strategy for avoiding the previously observed biaxial morphology, i.e. strain ramping which led to a reduced defect density and a well-aligned parallel lamellar structure [38]. Pinheiro and Winey [39] observed a mixed parallel–perpendicular lamellar morphology in a PS–PI diblock and a blend with PS homopolymer [39]. This structure was observed at temperatures between the parallel orientation, obtained following LAOS at low temperatures, and the perpendicular orientation obtained after high-temperature LAOS. The mixed morphology contained predominantly these two orthogonal states, but also intermediate orientations. The rheological response of the mixed state could be described by a linear combination of the responses for parallel and perpendicular orientations. It was noted that in between two critical frequencies for crossover of the dynamic elastic moduli (G' and G'' respectively) for parallel and perpendicular orientations, the orientation induced by LAOS corresponded to that which had the lower G' and G'' at the temperature and frequency of the strong shearing. The mixed morphology was obtained under conditions where the parallel orientation had a lower G' and the perpendicular orientation a lower G'' [39]. Using the rheometer with a shear sandwich developed for SAXS/rheology experiments by Hamley *et al* [40], Polis and coworkers investigated the process of lamellar rotation in a PS–PEP diblock pre-oriented into a parallel orientation by LAOS [41]. This suggested that the evolution of lamellar orientation during shear proceeds via lamellar rotation rather than through a discontinuous transformation, such as kink boundary migration or lamellar dissolution/reformation. In subsequent work, the rotation of kink bands and the lamellae within the kink bands was shown to occur continuously with increasing strain [42]. The nature of the kink band boundary as a function of strain was examined: chevron boundaries were found at low strains, and thus large tilt angles; however, at larger strains omega boundaries were formed which ultimately break (at large strains, $\sim$500%) [42]. Surface-induced orientation in a lamellar PS–PI diblock induced by LAOS has been probed by the same group using TEM and SAXS [43]. This indicated that a parallel orientation is formed at the surface, irrespective of bulk orientation.

The alignment of unoriented lamellae under extensional deformation has been investigated via SAXS, which revealed a transformation to a four-point pattern within the necked region of the sample [44]. It was suggested that necking occurs through local extension and contraction of the rubber phase with little ductile deformation of the glassy phase. The observed rotation of the four spots in the SAXS pattern was interpreted on the basis of intragrain shearing of lamellae, in which lamellar stacks orient along the stretching direction, although the lamellae within the stacks are tilted in a preferred direction [44]. The mechanical response of oriented lamellae, subjected to extension along the direction of the lamellar normal has recently been probed by SAXS and TEM for a poly(styrene)-poly(butadiene)–poly(styrene) (PS–PB–PS) triblock copolymer [45]. Contrary to theoretical predictions, an undulation instability was not associated with yielding of the sample above a (small) critical strain. Instead, the low strain behaviour (at ambient temperature, where PS is glassy) was found to be dominated by layers tilting in the vicinity of defects. This leads to the nucleation of a kink band, from which kink boundaries propagate parallel to the deformation direction, ultimately leading to the undulation of adjacent regions until folding into a chevron structure occurs. However, in the melt, the lamellae deformed affinely with the macroscopic elongation. The undulation instability was only observed near the glass transition of the PS, where both layers have significant viscoelasticity [45].

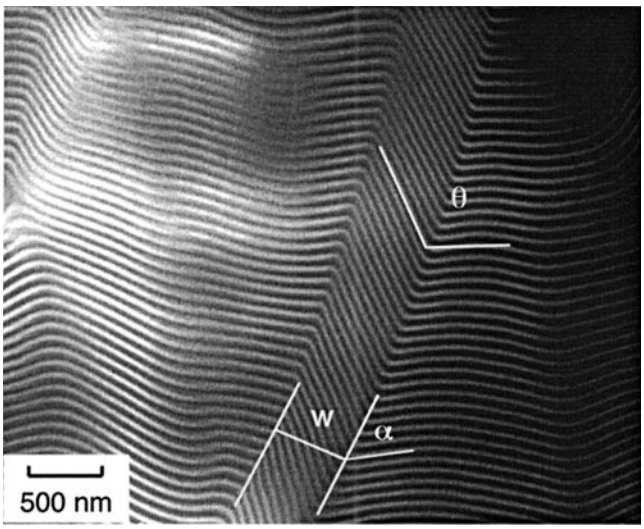

Figure 4. Transmission electron micrograph image of a forward kink band in a poly(styrene)–poly(ethylene-propylene) diblock subjected to steady shear [42].

A hexagonally perforated layer (HPL) phase, and a related hexagonally modulated lamellar (HML) phase were identified on the basis of SANS on a polyolefin diblock copolymer subject to a large-amplitude reciprocating shear [4, 46]. Both parallel and perpendicular lamellar states were accessed, the parallel orientation being obtained on heating from the low-temperature lamellar phase with high-strain, low-frequency shear. The perpendicular orientation was obtained under similar shearing conditions but on cooling from the disordered phase. By accessing both orientations, it was possible to probe the stacking of perforated/modulated layers under shear (perpendicular orientation) as well as the in-plane ordering of the perforations/modulations (parallel orientation). Subsequent work has shown that the HML phase is a transient phase that is unstable thermodynamically, whilst the HPL phase is a long-lived metastable structure [5, 15, 47].

For solutions of block copolymers, a convenient and widely used shearing geometry is the Couette cell. As illustrated in figure 5, depending on the direction of incidence of the x-ray or neutron beam two orthogonal planes can be probed. With the beam incident radially (i.e. along the shear gradient direction), the $(\boldsymbol{v}, \boldsymbol{e})$ plane is accessed. When the beam is incident tangentially, diffraction patterns can be recorded in the $(\nabla \boldsymbol{v}, \boldsymbol{e})$ plane. The effects of shearing the lamellar phase of a concentrated block copolymer solution in a Couette cell have been investigated using SANS [48, 49]. A solution of a PS–PI diblock in dioctyl phthalate (a neutral good solvent) was investigated and the lamellar orientation was monitored below and above the ODT temperature with the neutron beam incident either radially or tangentially to the Couette cell. It was found that below the quiescent ODT, oscillatory shear produced lamellae parallel to the plane of the shear cell walls. However, steady shear resulted in a reorientation of the lamellae into the perpendicular orientation (i.e. lamellar normals in the neutral direction) [49]. Above the transient ODT, the alignment induced by steady shear above a critical rate, quantified by the anisotropy of the scattering ring, was found to follow a master curve as a function of reduced shear rate (with respect to the shear rate for onset of orientation) for all temperatures [48, 49]. The critical shear rate was found to increase exponentially with temperature. The transition between parallel and perpendicular lamellar

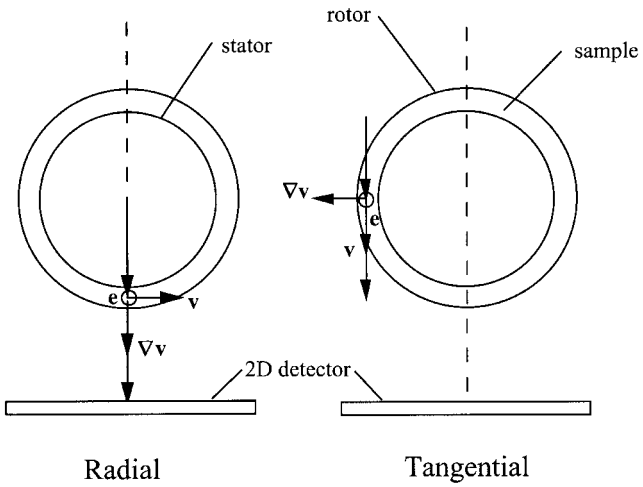

Figure 5. Scattering planes accessible when a beam is incident through a Couette cell (plan view). With the beam incident in the radial direction, the diffraction pattern in the (v, e) plane is recorded. In the tangential configuration, the diffraction pattern is recorded in the (∇v, e) plane.

orientations was probed in detail on a similar diblock solution subjected to oscillatory shear [50]. The transition between perpendicular and parallel orientation could be initiated at a fixed temperature by increasing frequency. A systematic difference in the defect density between parallel and perpendicular alignments was also noted. In particular, under shear flow a sample with parallel alignment was largely disordered due to a large number of defects, and it was pointed out that this shear-induced disordering below the quiescent ODT is not in agreement with existing theories [50].

A system with a disordered liquid phase at low temperature and a high-temperature lamellar mesophase was studied by Pople *et al* [51]. They performed SAXS experiments on a concentrated solution of a poly(ethylene oxide)–poly(butylene oxide) (PEO–PBO) diblock with *in situ* steady shearing. At low shear rates, a transverse lamellar orientation was observed, whereas at higher shear rates a transition to the perpendicular orientation was observed. The transverse orientation is the least favourable since the lamellar planes are perpendicular to the shear plane. Its observation in a diblock solution may be due to a trapped non-equilibrium state resulting from the sample mounting procedure. This orientation has been observed following the abrupt cessation of large-amplitude reciprocating shear in the disordered phase of a pentablock copolymer melt [52], and rationalized on the basis that chain orientation along v overwhelms the penalty for lamellar interfaces perpendicular to the flow direction.

In aqueous solutions of the Pluronic triblock copolymer P85 ($PEO_{25}PPO_{40}PEO_{25}$, PPO = poly(propylene oxide)) forming a lamellar phase, Mortensen has reported that following shear, parallel and perpendicular orientations coexist with all other lamellar orientations in which layers are parallel to the flow direction [53]. A transition from parallel to perpendicular lamellae on increasing shear rate was observed for concentrated solutions of Pluronic triblocks P123 ($PEO_{20}PPO_{70}PEO_{20}$) [54] and F127 ($PEO_{100}PPO_{70}PEO_{100}$) [54, 55] in butanol/water mixtures. Samples were subjected to steady shear in a Couette cell, and investigated by SANS. At lower concentrations of the same system, shear-induced formation of multilamellar vesicles (onions) (figure 6) was observed, based on SANS patterns in radial and tangential geometries and additional small-angle light scattering data, which showed a four-lobe pattern characteristic of spherulites (vesicles) [54, 55]. The transition to onions was also characterized by shear

thickening behaviour, whereas the viscosity decreased across the parallel-to-perpendicular transition in the more concentrated solution [54].

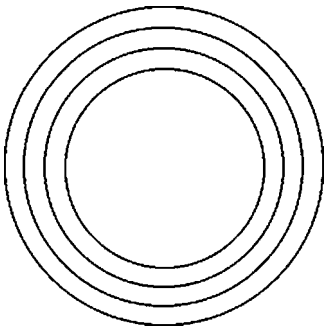

Figure 6. Schematic diagram of a multiplayer vesicle ('onion').

In the lamellar systems discussed so far, the layers consist of amorphous polymers. In contrast, a system containing crystalline poly(ethylene) has been investigated by Richter *et al* [56]. They observed needle-like lamellar aggregates in solutions of semicrystalline poly(ethylene)–poly(ethylene–propylene) diblocks in decane. The poly(ethylene) crystallized in lamellar platelets, surrounded by poly(ethylene–propylene) 'brushes'. Shear orientation caused the needle-like lamellar aggregates to orient with their long axes along the shear direction, but random orientation about this direction. This was confirmed by SANS on samples sheared between two parallel quartz plates: following orientation, the cell was rotated with respect to the neutron beam to map out the three-dimensional structure. SANS with *in situ* shearing on the same samples in a Couette cell confirmed orientation of lamellae up to a shear rate above which an isotropic pattern was observed, suggesting the occurrence of shear melting [56].

3. Hexagonal phase

The hex phase was the first block copolymer morphology to be oriented by flow. In pioneering work, Keller and coworkers [18, 20] demonstrated that extrusion could be used to macroscopically align cylindrical microdomains in a PS–PB–PS triblock copolymer. Micrographs from this copolymer (Kraton 102, now D1102, 25 wt% PS content) are reproduced here (in figure 7); when viewed end-on the hexagonal arrangement of the rods is obvious, and when viewed from the side the layers of cylinders are evident.

The first studies to show the effect of reciprocating shear on a block copolymer were performed on the hex phase of a PS–PB–PS triblock by Hadziioannou *et al* [57, 58]. They demonstrated using SAXS that 'monodomain' specimens could be prepared by reciprocating planar shear. Almdal *et al* [59] showed that LAOS can be used to prepare well-oriented domains of the hex phase, by performing SANS on a presheared PEP–PEE diblock. For the PEP–PEE system, it has been found that polymers with $f_{PEP} > 0.5$ exhibit excellent ordering, although samples with $f_{PEP} < 0.5$ are difficult to align. Since PEP has a lower entanglement molecular weight than PEE, it follows that stiff cylinders in a soft matrix are harder to align than the reverse structure [21].

Morrison and coworkers [60] used SANS to probe the effect of shear on an asymmetric PS–PB–PS triblock forming a hex phase. The same polymer was used by Nakatani *et al* [61] to determine the effect of shear on the ODT and Winter *et al* [62] used SAXS to confirm the

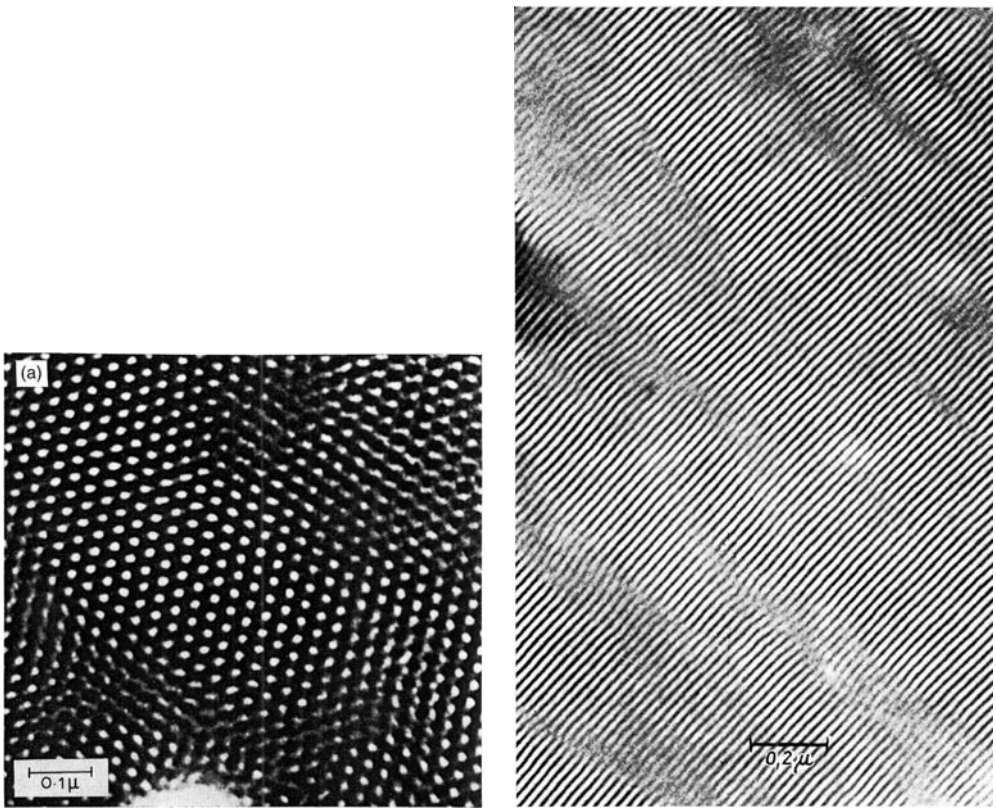

Figure 7. TEM micrographs from a hex phase subject to flow during extrusion. The sample was a PS–PB–PS triblock (Kraton D1102) [128]: (a) perpendicular to the extrusion direction and (b) a parallel section.

orientation induced by large-amplitude oscillatory Couette shear in a PS–PI–PS triblock.

A common feature of the alignment induced in lam and hex phases by LAOS was noted by Tepe *et al* [63]. They reported that a 'perpendicular' orientation of cylinders in a polyolefin diblock, with (10) planes perpendicular to the shear plane, could be attained by shearing near the ODT, whereas shearing well below the ODT led to a parallel orientation of (10) planes with respect to the shear plane [63]. The latter is the orientation obtained most usually.

Bates and coworkers [64] suggested that the hex-disorder transition of previously sheared cylinders proceeds via a transient undulating cylinder or bcc spherical state (see figure 8). This was supported by the observation of the development of azimuthal peaks as a function of time in the SANS pattern at a fixed temperature in the disordered phase, following cessation of shear which stabilized the hex phase. The thermally-induced transition from a thermodynamically metastable hex phase trapped by solvent casting to the stable lamellar phase in a PS–PB–PS triblock was studied by Sakurai *et al* [65]. On the basis of SAXS and TEM, they suggest that this transition occurs via the coalescence of undulating cylinders.

A martensitic-like phase transition in a hex-phase-forming PS–PB–PS triblock melt subjected to steady shear was proposed by Jackson *et al* [66]. For samples under shear in the Couette cell, they observed the development of a higher-order Bragg peak along the neutral direction at a position $\sqrt{3}q^*$ in the SANS patterns in the $(\boldsymbol{v}, \boldsymbol{e})$ plane. Hexagonal

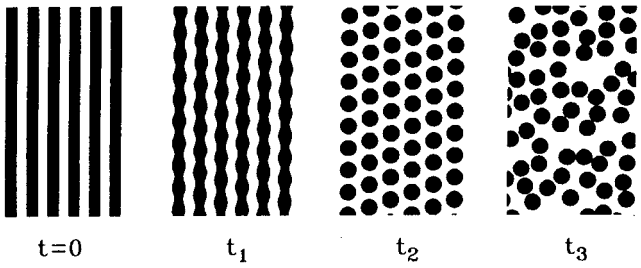

Figure 8. Schematic representation of the transition from cylinders to disorder following cessation of large-amplitude shear, deduced from SANS experiments on an asymmetric PEP–PEE diblock [64]. Shear was used to stabilize a hex phase above the equilibrium ODT, and the relaxation back to the equilibrium disordered phase was followed after the shear was stopped.

ordering was confirmed from SANS patterns in the $(\nabla \boldsymbol{v}, \boldsymbol{e})$ plane, which revealed preferential orientation of (10) planes in the shear plane. The presence of the higher-order reflections was suggested to be due to grains of cylinders with a smaller diameter and packed in a lower symmetry arrangement (spacegroup $p3m1$ instead of the $p31m$ spacegroup for hexagonal-packed cylinders). However, a simpler explanation of the development of the peak at $\sqrt{3}q^*$ is incomplete orientation of (10) lattice planes in the shear plane, since (11) planes give rise to a Bragg peak at this position [67]. The TEM evidence presented by Jackson *et al* may simply reflect artefacts from the ultramicrotoming procedure.

A number of studies have focused on the effects of extensional deformation on the structure and mechanical properties of triblock copolymers forming hex phases, in particular of the ABA type with poly(styrene) end blocks (glassy at room temperature) and either poly(butadiene) or poly(isoprene) as rubbery midblocks. Following their early TEM and SAXS studies of orientation induced by extrusion, Folkes, Keller and coworkers examined the deformation behaviour of PS–PB–PS (Kraton^{TM}-type) triblocks. The anisotropy of the Young's modulus was analysed by Arridge and Folkes [68], and compared to theories for fibre-reinforced composites of hexagonal symmetry. Later, the deformation behaviour at large extensional strains was investigated via stress–strain measurements, SAXS, TEM and birefringence [69]. Samples subjected to tensile strain either perpendicular or parallel to the axis of the cylinders were investigated. For deformation perpendicular to the cylinders, the deformation was affine up to about 20% strain (later work on a lower molar mass sample found affine behaviour up to 45% strain [70]). At higher strains time-dependent irreversible deformation was observed, due to cracking along crystallographically defined directions of the hexagonal lattice. For tensile strain parallel to the cylinders, yielding was observed at only 3% strain. A closer inspection of the sample revealed that the deformation in the necked region reached 80% before the neck spread across the sample. This was suggested to be due to the breakup of PS cylinders, as confirmed by TEM experiments, which showed the existence of short PS cylinders in a strained sample. The observed yielding behaviour was interpreted using models for fibre-reinforced composites, including one based on randomly broken cylinders which gave values in agreement with those obtained from TEM images [69].

The behaviour of a PS–PB–PS sample hex phase subjected to large extensional strains both parallel and perpendicular to the cylinder axis was investigated via SAXS by Tarasov *et al* [71]. Stretching parallel to the cylinder axis was found to lead to fracture of the cylinders into 100 nm long rods, as in the TEM study of a similar sample by Odell and Keller [69]. However, tensile deformation perpendicular to the cylinder axis led to buckling of the PS rods, as indicated by the splitting of meridional Bragg peaks from layers of cylinders into a characteristic 'four-

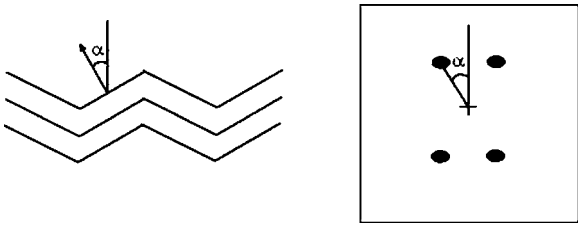

Figure 9. Illustrating the buckling of cylinders (viewed edge on), along with the accompanying 'four point' small-angle scattering pattern.

point' pattern (figure 9). The angle of the peaks with respect to the stretching direction was found to increase with strain. A later study [72] of the tensile deformation of Kraton-type block copolymers using SAXS found that deforming cylinders parallel, perpendicular or at an intermediate angle (45°) with respect to the stretching direction results in buckling of cylinders, as shown by four-point scattering patterns at large (>100%) strains. In the perpendicular direction, the domain spacing increased as the sample was stretched and the deformation was affine at low strains. At about 170% strain, however, a second set of reflections indicated that some domains had relaxed into their original unstretched spacing. In the parallel orientation the deformation was affine, even above the yield point (110% strain) and necking was not observed [72].

Well-oriented domains of PS–PI–PS triblocks can be obtained via the roll-casting technique, where the polymer dissolved in solvent is squeezed between counter-rotating cylinders whilst the solvent is allowed to evaporate. The high degree of alignment attained was confirmed via TEM and SAXS [22]. The perpendicular deformation of samples prepared in this way (to produce 'near single crystals') has recently been investigated in considerable detail, via SAXS [73] and TEM [74] with *in situ* measurement of load and displacement. SAXS indicated that the deformation proceeded in two stages. In the first, the deformation was nearly affine up to approximately 100% strain. The rubber matrix extended along the stretching direction while contraction occurred almost exclusively along the neutral direction due to the constraint imposed by the aligned PS cylinders. The measured Poisson's ratio of 0.9 compared well to the value expected (1.0). Above 130% strain, kinking of oriented cylinders into a buckled state was inferred from four-point patterns obtained from SAXS patterns using the x-ray beam at perpendicular incidence, and from distortions in the initially hexagonal SAXS pattern at parallel incidence. A companion paper examines deformation mechanisms in real space via TEM [74]. An interesting feature of this work was the technique of cross-linking the isoprene block via electron beam irradiation to fix the morphology in a particular deformation state for examination by TEM. TEM sections parallel to the cylinder axis revealed that the initial hexagonal packing of the cylinder distorted into a faulted twinlike texture in which layers of cylinders were oriented at fixed angles with respect to the stretching direction. Perpendicular sections provided direct evidence for a chevron texture of cylinders with symmetric kink boundaries. These observations were combined into a 3D model for the deformed morphology [74].

The mechanical properties and structure under deformation of ABA triblocks containing a rubbery midblock (B ≡ poly(ethylene-co-butylene)) and glassy endblocks (A ≡ poly(styrene)) have been investigated in a series of publications by Hamley and coworkers [75]. These materials are Kraton copolymers in which the midblock is hydrogenated poly(butadiene). SAXS experiments were performed on samples oriented by compression moulding, with oscillatory extensional strains applied both parallel and perpendicular to the cylinders [75].

The SAXS data acquisition was synchronized to the applied sinusoidal wave, so that changes in the inter-cylinder separation (from q^*) could be correlated to the applied strain with a time resolution of 2 ms. It was found that the lattice deformed in phase with the applied strain, although in a non-affine fashion even though the strain amplitude was only 7%. The observed change in domain spacing for the cylinders was significantly smaller than the applied strain for both perpendicular and parallel orientations. The deviation from affine behaviour was greatest for the parallel orientation. The non-affine behaviour was ascribed to the take-up of strain by initially poorly oriented grains. These results differ from those obtained from PS–PB–PS triblocks subjected to tensile deformation (where affine deformation was observed for larger strains), due to differences in the type of deformation and in the elasticity of the midblock.

The effect of planar extension on a similar Kraton triblock was examined using SANS for a pre-oriented sample subjected to uniaxial extension parallel to the cylinder axis [76]. The reduction in inter-cylinder spacing was found to be non-affine, above the yield stress (5%). The change in shape of the SANS peaks arising from the planes of the cylinders was consistent with the mechanism put forward by Pakula *et al* [72], i.e. 'micronecking' and subsequent breaking of cylinders at higher strains (figure 10), without any change in domain spacing [76]. Extensional rheometry has been used to examine the anisotropy of mechanical properties of the same triblock, in combination with shear rheometry above the poly(styrene) glass transition temperature [77]. Measurements of the extensional dynamic modulus E revealed that below the PS block glass transition temperature pre-oriented triblocks show highly anisotropic mechanical properties, with the storage modulus E' higher along the flow direction than perpendicular to it. Above the PS glass transition temperature the anisotropy in E vanished. Samples in this molten state were investigated via oscillatory shear rheometry. At high frequency, the mechanical response was found to be independent of orientation while at low frequencies the storage modulus was found to be lower along the flow direction than perpendicular to it. This was explained by the ability of the PS blocks to relax more easily along the flow direction [77].

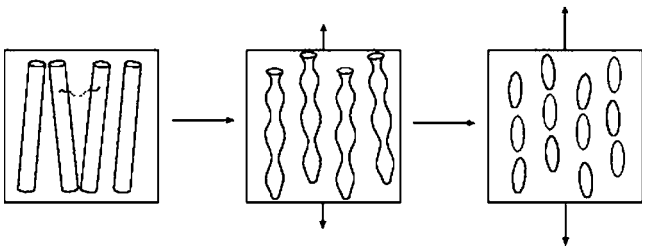

Figure 10. Schematic diagram of the structural transformations accompanying the non-affine deformation of a hex phase of glassy cylinders in a rubbery matrix under extension [76]: left, undeformed; centre, correlated 'micronecking' (undulations) of cylinders; and right, break-up of cylinders.

Shear has been shown to influence the ODT of block copolymer solutions, as well as melts. Balsara *et al* [78] observed a significantly higher disordering transition temperature for a PS–PI diblock in the nearly neutral solvent dioctyl phthalate oriented by steady shear compared to polydomain samples prepared under quiescent conditions. In sheared polydomain samples where the imperfections were partially removed, coexistence of ordered and disordered regions was observed at temperatures between the two limiting ordering transition temperatures. However, these observations have not been satisfactorily accounted for.

A transition from shear-induced order to shear-induced disorder at higher shear rates has

been reported above the quiescent ODT in the same system [79]. The samples were investigated by SANS with *in situ* steady shear. It was pointed out that existing theories for the effects of shear on block copolymers only predict shear-induced ordering due to the suppression of composition fluctuations. However, it was proposed that fluctuations of the cylinders, if characterized by a lifetime larger than the inverse shear rate, lead to the disordering observed at high shear rates.

Shear orientation of the hex phase formed in aqueous solutions of Pluronic P85 ($PEO_{25}PPO_{40}PEO_{25}$) confirmed the long-range nature of the induced alignment [53]. A sample was sheared between parallel plates and investigated using SANS, by rotating it with respect to the neutron beam. With the neutron beam incident along the shear gradient direction, a SANS pattern with a pair of meridional Bragg reflections was observed, showing orientation of the cylinders along the shear direction. The hexagonal order was confirmed by the six-fold symmetry of the SANS pattern with the neutron beam along the shear direction. At lower concentrations of this triblock, shear orientation of rodlike micelles leads to an aligned nematic phase [53].

The effect of LAOS on the orientation of a hexagonal phase formed in solutions of $PEO_{18}PBO_{10}$ in 0.2M K_2SO_4 has been studied using SAXS on samples subjected to steady shear in a Couette cell [80]. The orientation was quantified in terms of order parameters $\bar{P}_2$, $\bar{P}_4$ and $\bar{P}_6$, where $\bar{P}_n$ denotes an ensemble-averaged Legendre polynomial of order n. These order parameters were extracted from the SAXS patterns using a model of the scattering from oriented infinitely long cylinders. It was found that the order parameters increased logarithmically with the shear rate. A limiting degree of orientation with $\bar{P}_2 \sim 0.6$ was reached at a shear rate $\dot{\gamma} = 100\ s^{-1}$, above which an increase in shear rate did not significantly improve the orientation. Time-resolved SAXS experiments revealed that a steady-state degree of alignment developed in the gel over a timescale, $t \sim 30$ s; however, upon cessation of shear partial loss of orientation was observed with $t \sim 1$ h [80]. A related study was undertaken for aqueous gels of $E_{40}B_{10}$ [81]. Here, it was shown that the susceptibility to shear orientation depended on diblock concentration, because a gel containing 25% diblock did not shear orient, whereas gels containing between 30–38% diblock did form a shear-oriented cylindrical structure. In that work, simultaneous SAXS/rheology experiments were supplemented by SAXS measurements on gels sheared *in situ* using a Couette cell in order to probe slow relaxation processes. It was thus shown that whereas the dynamic shear moduli recovered within 30 s to their original values upon cessation of shear, partial orientation of the gel structure was retained for over 1 h [81]. However, in contrast to the $E_{18}B_{10}$ solution, all orientation was lost in this gel after 2 h relaxation.

4. Cubic micellar phases

The macroscopic alignment of a body-centred cubic (bcc) phase induced by LAOS has been probed using SANS. Almdal *et al* [83] sheared a PEP–PEE diblock with a volume fraction $f_{PEP} = 0.83$ using a custom-made shear machine; the resulting oriented sheet was then cut into three orthogonal planes. SANS patterns were obtained from these three projections of the structure and a twinned bcc structure was found to be consistent with the data. The twinned bcc structure is illustrated in figure 11. The slip plane was found to be the (110) plane, coincident with the shear plane with the $[\bar{1}11]$ slip direction coincident with the shear direction. This is one of the principal slip systems for bcc metals, and a similar orientation was also observed for colloidal suspensions under steady shear as noted by Koppi *et al* [67]. The {110} planes are the most widely spaced, and the ⟨111⟩ directions are the closest packed directions.

The epitaxial growth of a bcc phase on heating the hex phase of the same diblock copolymer

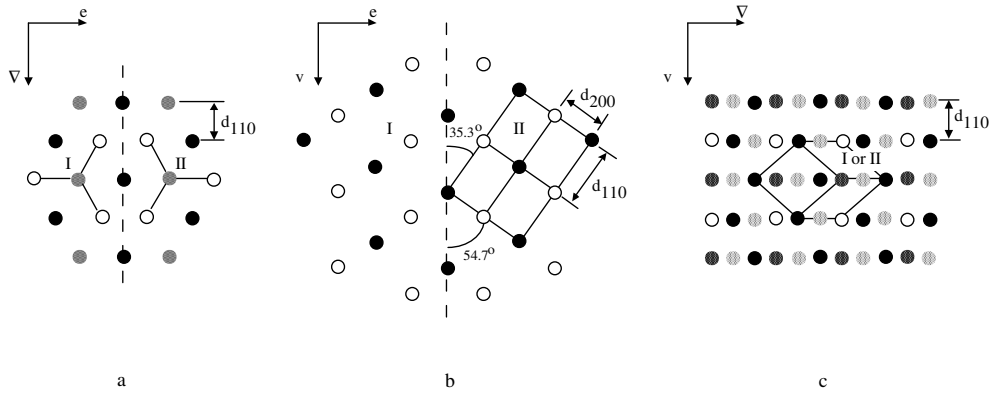

Figure 11. Projections of the twinned bcc structure observed for a sheared polyolefin diblock copolymer melt [83]. Twins I and II are indicated, as are interplanar spacings, d (modified from figure 3 in [83]).

(and another with a minority phase of PEP) was investigated by Koppi *et al* [67]. The low-temperature hex phase was oriented by reciprocating shear and then the sample was heated into the bcc phase in the absence of shear. It was observed that twinned bcc structures grow epitaxially from the hex phase, with the [111] direction in the bcc structure coincident with the original cylinder axis. Deformation of the bcc phase under shear resulted in different responses depending on the shear rate relative to the inverse relaxation time of the defects, as illustrated in figure 12. At low shear rates the crystal orientation is preserved, and bcc spheres slip via creep: {110} planes move along the $[\bar{1}11]$ (shear) direction. At intermediate shear rates, the sample apparently becomes disordered, giving isotropic SANS patterns. However, after cessation of shear the twinned bcc structure reappears. These results indicate that at intermediate shear rates the {110} planes lose translational order whilst maintaining orientational order. This loss of translational order was ascribed to defects being generated at a rate faster than that at which they can be annihilated; this occurred above a critical shear rate γ^*. At higher shear rates, the deformation rate exceeds the time required for defect formation. Then large-scale elastic deformation can occur in these soft materials rather than the fracture that would be expected in metals. This is probably achieved as an affine, elastic deformation of spheres within the lattice planes, as illustrated in figure 12. Removal of the shear field then causes the spheres to return to their original shape [67].

Simultaneous SAXS/rheology measurements were performed for the bcc phase of a PS–PEP diblock containing PS spheres in the low-temperature, strong segregation regime by Okamoto *et al* [82]. LAOS induced preferential orientation of the {110} planes in the plane defined by the shear and vorticity directions. The stress amplitude was found to decay with the number of strain cycles and stress recovery was observed after the cessation of shear. They also investigated the dynamic response of the bcc lattice during a single cycle of shear and found that meridional [110] reflections were fixed in position, whereas the position of $\bar{1}10$ reflections varied depending on the strain phase. This was ascribed to the dynamic deformation of the bcc lattice. The applied strain and the strain on the lattice were found to be out of phase. In contrast to the results of Almdal *et al* [83] the orientation of the {110} planes was found to relax completely upon cessation of shear [82]. In subsequent time-resolved synchrotron SAXS experiments the orientation under LAOS was investigated for a PS–PEP diblock of inverse composition, i.e. soft PEP spheres in a more rigid PS matrix [84]. This also

differs from the bcc-forming PEP–PEE diblocks studied by the Bates group [67, 83], where both components are rubbery. The measurements by Shin *et al* [84] were performed at two temperatures above the PS glass transition, and well below the ODT. The initial orientation of the sample was created during uniaxial compression. The lattice periodicity was obtained from Bragg reflections, whilst information on the strain-induced distortion of the PEP spheres was inferred from changes in the shape of the amorphous ring arising from the sphere form factor (a distortion from a circle into an ellipse was observed under strain). The lattice was found to deform almost affinely and in phase with the macroscopic strain. The spheres also deformed in phase with the strain, although only to about 50% of the applied strain, probably due to the large energy penalty for distorting spheres even when they are softer than the matrix. The dependence of the local lattice strain, $\gamma_{lattice}$, or sphere strain on strain cycle N was examined. Both were found to decay with N, although $\gamma_{lattice}$ decayed faster. Lissajous patterns of stress *versus* strain acquired simultaneously with the SAXS data showed an increase in nonlinear viscoelastic behaviour with N. However, under the conditions of applied LAOS, macroscopic alignment of the lattice was not induced, i.e. the initial orientation was recovered at the zero strain phase of each cycle of LAOS. The lattice deformed with increasing strain but the deformation and orientation were lost as the strain decreased [84].

A number of studies have focused on the effect of deformation on the microstructure of block copolymers forming poly(styrene) spheres in a rubbery matrix [85–7]. The orientation of a poly(styrene)–poly(isoprene) diblock in mineral oil induced by roll-casting has been investigated using SAXS [87]. Inoue *et al* [85] investigated the effect of uniaxial extension on the orientation of PS–PI and PS–PI–PS copolymers using SAXS and light scattering. They observed that the lattice deformation was affine with the applied strain at small strains, but at larger strains microvoid formation led to density inhomogeneities. The deformation of the PI midblock in a PS–PI–PS triblock subjected to uniaxial strain has been studied using SANS with contrast matching using a deuterated midblock [86]. The PS–PI diblock examined by Prasman and Thomas [87] was found to orient with a [111] direction along the flow (rolling) direction.

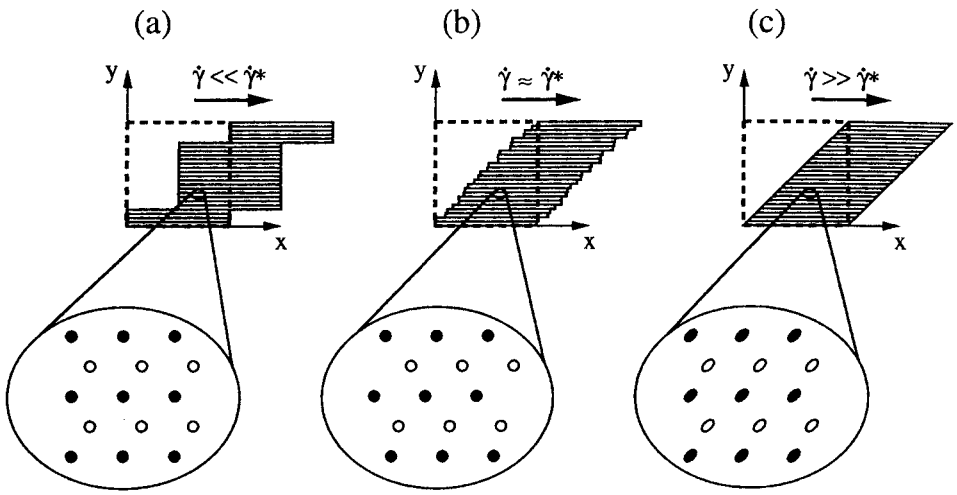

Figure 12. Three deformation mechanisms proposed for bcc spheres, depending on shear rate [67]: (a) slow shearing results in creep; (b) at an intermediate shear rate, the generation of numerous defects leads to a loss of translational order; and (c) at high shear rates, the spheres undergo an affine elastic deformation. The layers shown represent {110} planes of a bcc structure. γ^* is the inverse relaxation time of the defects.

The lattice deformed affinely with the macroscopic deformation up to 300% strain. The location of the first minimum in the form factor in the SAXS patterns also remained essentially unchanged up to this strain, indicating that the glassy PS domains retained their spherical shape [87]. SANS on a pre-oriented Kraton PS–PEB–PS triblock subjected to *in situ* uniaxial extension revealed an affine (and reversible) deformation process (up to 63% strain) [76]. The sample was initially oriented by compression in a channel die, which is the equivalent of planar extension, and led to orientation of the bcc phase with a [111] direction along the flow direction. The structural anisotropy led to pronounced mechanical anisotropy, as exemplified by stress–strain curves for stretching of samples with different orientations relative to the channel die flow direction. SANS data indicated that the domain spacing decreased perpendicular to the extension direction, although there was a corresponding increase in inter-sphere spacing along this direction. At the highest strains, a de-correlation between 'strings' of spheres along the extension direction was inferred [76].

The effect of steady shear on gels formed by a poly(styrene)–poly(ethylene-propylene) diblock in dodecane (a selective solvent for the latter block) was investigated using SANS by Higgins and coworkers [88, 89]. It was found that long-range order was induced by very low shear rates, whereas shear melting was noted at high shear rates [89]. The data were interpreted on the basis of a distorted fcc structure, with an ABCABC... stacking of hexagonal close-packed layers (figure 13(a)) but distorted from a close-packed arrangement due to normal stresses [89].

The effect of steady shear in creating long-range order in cubic gel phases formed by PS–PI diblocks in decane has been investigated using SANS [90]. Both bcc and fcc phases were observed depending on the copolymer composition and concentration. For the fcc structure, a transition from polycrystallinity to sliding hexagonal close-packed (hcp) layers was observed on increasing the shear rate. As the shear rate increased, the layers did not hop perfectly from one registry site to the next, i.e. zig-zag motion (figure 13(b)) was not observed. Instead they slid over one another (figure 13(c)). Examples of SANS patterns obtained on increasing shear rate are shown in figure 14. The bcc crystals were observed to gradually orient into a twinned bcc structure, with the {110} planes normal to the shear gradient direction. The bcc twins were observed to slip along the twinning planes, allowing the crystal to flow at moderate shear rates. At higher shear rates, a loss of long-range order associated with shear melting of the bcc structure was observed. The diffraction patterns from ordered bcc and fcc crystals were modelled in detail using theory developed by Loose and Ackerson [91] for layered structures in colloidal dispersions. Examples for the fcc phase are shown in figure 15, where the model was optimized to obtain qualitatively similar diffraction patterns to the experimental ones at different shear rates shown in figure 14. Shearing was also used to identify bcc and fcc structures in PS–PI diblock solutions in decane, as part of a study of the effect of copolymer concentration on micellar ordering. Here, highly oriented SAXS patterns were obtained simply by hand shearing of the gels between sliding parallel plates [92].

A twinned bcc structure was identified in a gel of a commercial thermoplastic elastomer triblock copolymer using SANS on a sample subjected to oscillatory strain in a modified rheometer [93]. The gel was formed from a PS–PEB–PS Kraton^{TM}-type copolymer in extender oil (a mixture of aliphatic and acyclic compounds that is a selective solvent for the midblock). These gels can also be stretched to yield oriented micellar gels, and the effect of extensional strain on the gel structure has been probed by SANS [94, 95].

The effect of shear on cubic gels formed by PEO–PPO–PEO (Pluronic) copolymers has been investigated using SANS by Mortensen and coworkers, for samples subjected to steady shear in a Couette cell [53, 96–8]. In both $PEO_{25}PPO_{40}PEO_{25}$ (Pluronic P85) [96] and $PEO_{97}PPO_{39}PEO_{97}$ (Pluronic F88) [97, 98], a bcc phase was identified. SAXS has also

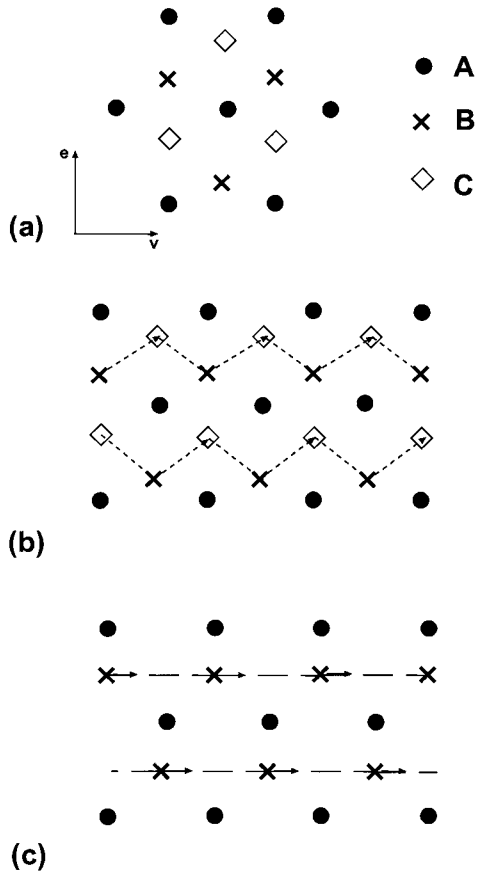

Figure 13. (a) ABCABC stacking sequence of hexagonal close-packed (hcp) layers in an fcc phase. (b) Zigzag motion of a hcp layer (×) with respect to a reference layer (●) [91]. (c) Sliding motion of two neighbouring layers [91].

been used to elucidate the complex rheology found in solutions of F68 ($PEO_{76}PPO_{29}PEO_{76}$) forming a bcc phase [99]. The flow in a Couette cell was inhomogeneous due to the large stress gradient (a decrease of 20% at the outer wall compared to the inner wall). Two successive orientation transitions were observed to occur at very different shear rates but separated by a narrow difference in stress. The stress as a function of shear rate shows two plateaus (figure 16), within each of which two distinct structural organizations coexist in the gap of the Couette cell. This phenomenon has been termed 'shear banding' and had been observed earlier for sheared solutions of wormlike micelles. The structure of the gel as a function of shear rate was elucidated by SAXS. This revealed that at low shear rates, a viscous polycrystalline state filled the gap. At intermediate rates, a first oriented state was observed with {211} planes parallel to the shear plane. The proportion of this state increased across the first stress plateau. At higher rates, in the second plateau, a second oriented state was observed with {110} planes oriented in the shear plane. These two sets of planes are illustrated in figure 17. Flow at shear rates corresponding to the second plateau occurs via the layer sliding mechanism, observed earlier for highly charged colloidal latex suspensions [100] and illustrated in figure 13(c). In both oriented states, the close-packed ⟨111⟩ direction was along the shear direction. Because

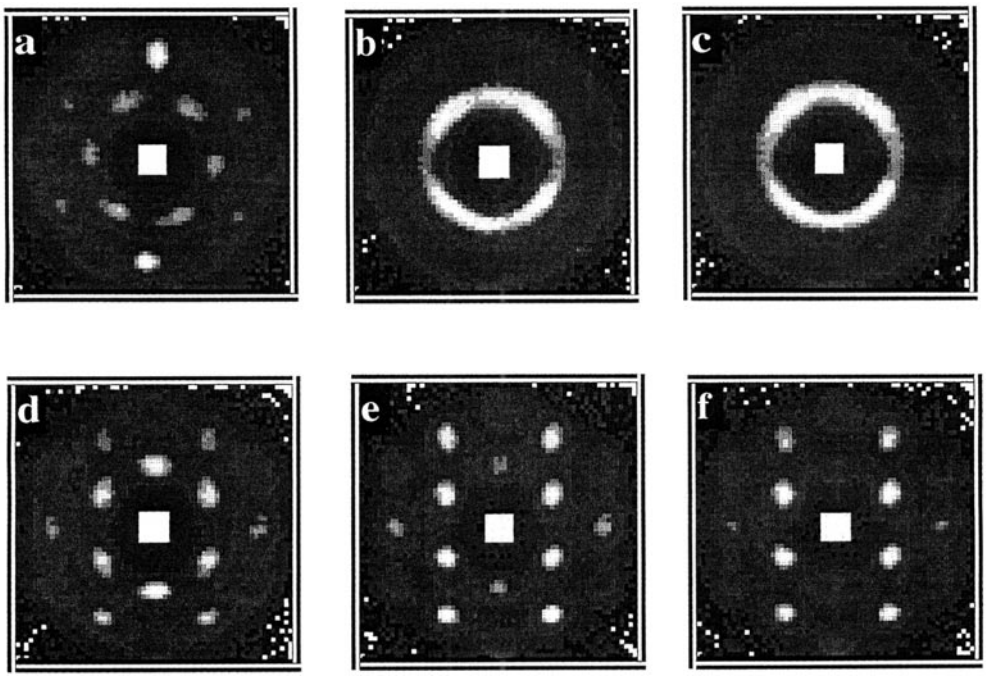

Figure 14. SANS patterns obtained for a fcc gel containing 15% of a PS–PI diblock (M_w = 55 000 g mol^{-1}, 60 wt% PS) in decane [90] and subjected to steady shear at different shear rates: (a) $\dot{\gamma} = 0$, aligned by inserting stator of Couette cell; (b) $\dot{\gamma} = 0.06$ s^{-1}; (c) $\dot{\gamma} = 0.66$ s^{-1}; (d) $\dot{\gamma} = 6.60$ s^{-1}; (e) $\dot{\gamma} = 66.0$ s^{-1}; and (f) $\dot{\gamma} = 200.0$ s^{-1}. In these patterns, q ranges from -0.028 to $+0.028$ Å^{-1} and the shear direction is horizontal.

the stress gradient in the Couette cell (20%) was larger than the 2.5% difference in stress separating the two plateaus in the rheology data (figure 16), the intermediate state with {211} planes parallel to the shear plane was never observed in isolation, but only in combination with the disoriented state (at $\dot{\gamma} = 16$ s^{-1}) or with the layer-sliding state (at $\dot{\gamma} = 160$ s^{-1}). Scanning the x-ray beam across the gap of the Couette cell confirmed that the intermediate orientation state was located close to the outer wall, as expected since the stress was lower there.

A question remains as to why stress plateaux were not observed for an fcc gel formed in a related PEO–PPO–PEO copolymer (Pluronic F108) studied via creep rheometry by Eiser *et al* [101], despite the observation of strong shear thinning. The difference compared to the bcc gel in $PEO_{76}PPO_{30}PEO_{76}$ could be because no purely elastic regime was observed for the fcc gel, suggesting a high density of dislocations sufficient to induce flow even for small, applied stresses. The bcc gel may be less defective, alternatively there may be a difference due to the distinct preferred flow planes in bcc compared to fcc gels. Hamley and coworkers [102] have also compared the flow behaviour of fcc and bcc gels subjected to LAOS, and also noted the much more elastic response of the bcc gel. In a bcc gel the flow appears to be hindered resulting in a slip-stick motion as planes of micelles shear past one another. In contrast, in a fcc gel sliding of hcp layers appears to be unhindered (at least at sufficiently high shear rates). This difference may reflect the difference in the intermicellar potential, which is more long range in the case of a bcc packing of micelles. A single plateau in shear stress versus shear rate has also been observed for a PEO–PBO diblock in water and this was ascribed to inhomogeneous flow, possibly shear banding [103]. SAXS revealed that flow in the plateau region occurred in

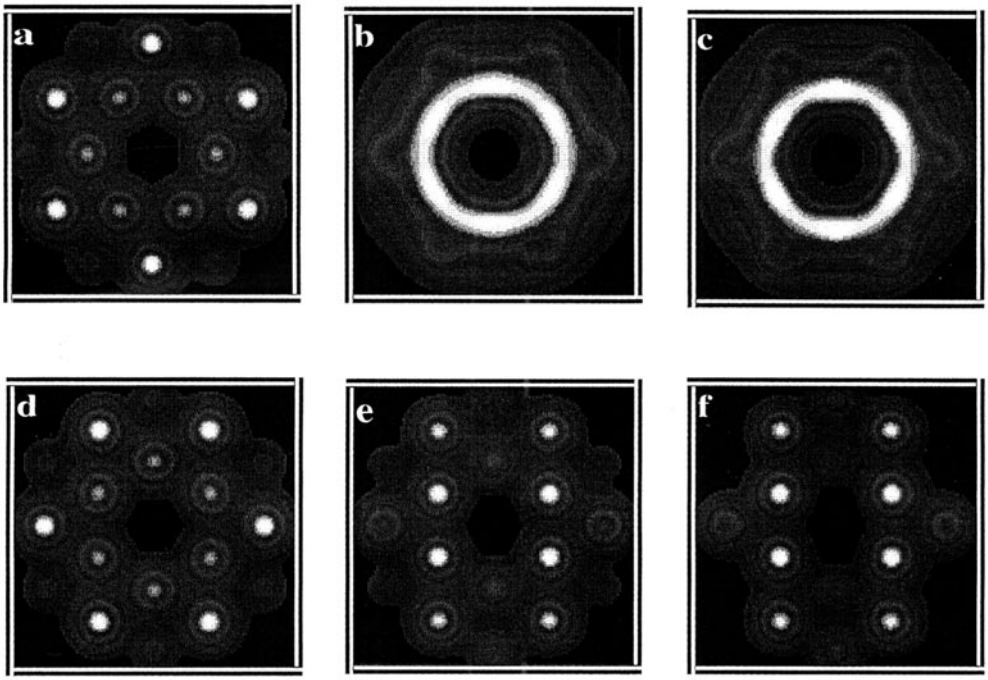

Figure 15. Models of the fcc phase under shear using the Loose–Ackerson model [91] optimized to correspond to patterns in figure 3 [90].

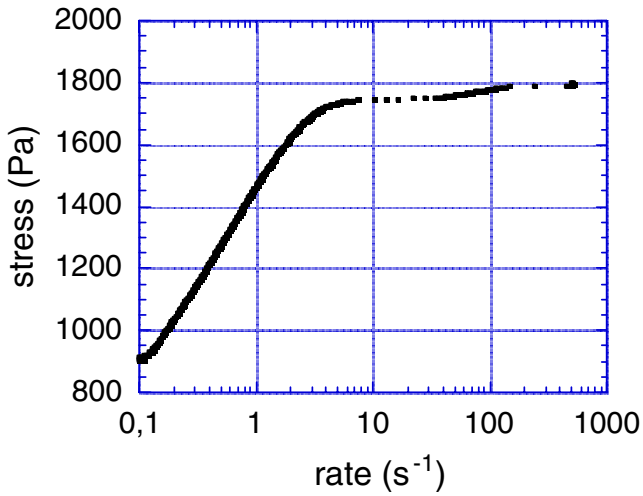

Figure 16. Two plateaux observed when stress is measured as a function of shear rate for a 46 wt% gel of $PEO_{76}PPO_{29}PEO_{76}$ in water, which forms a bcc phase [99].

{110} planes with a close-packed [111] direction along the shear direction. However, at higher shear rates flow occurred with the {110} and {211} planes oriented in the shear plane. It is not clear why these flow mechanisms are distinct from those observed by Eiser *et al* [99], but there are differences in the copolymer architecture (triblock *versus* diblock) as well as the gradient

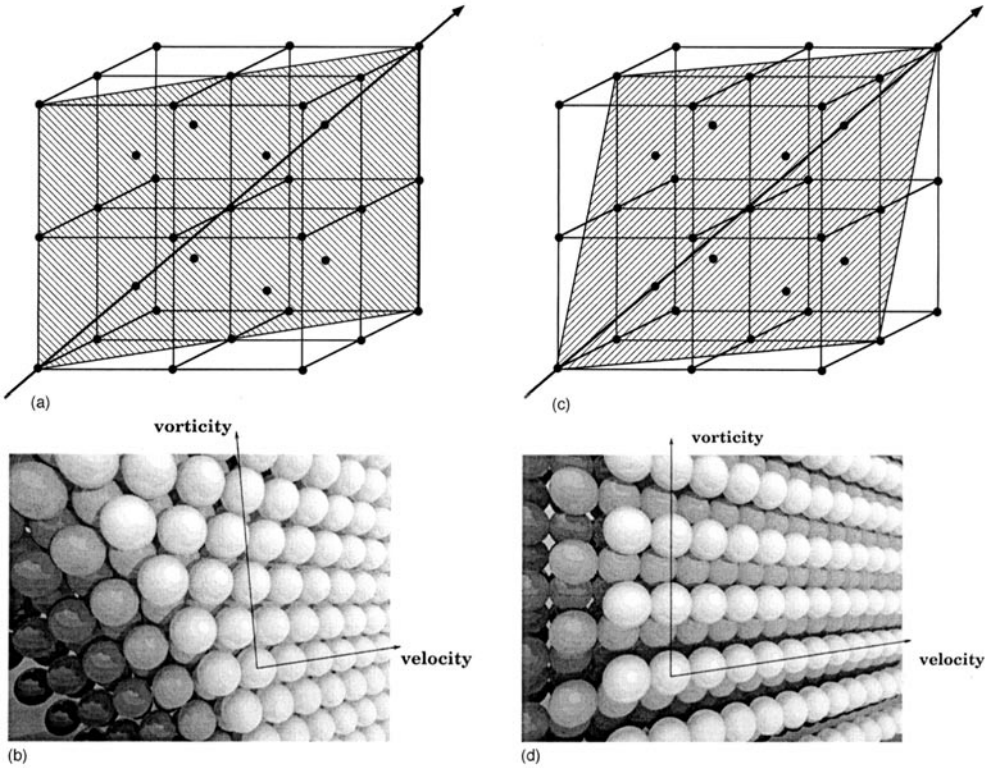

Figure 17. Flow planes in a bcc lattice [99]: (a) bcc lattice with a {110} plane shaded; (b) section of a bcc lattice showing a {110} plane; (c) bcc lattice with a {211} plane shaded; and (d) section of a bcc lattice showing a {211} plane.

in shear velocity [103].

Shear-induced orientation effects in fcc structures have been examined in detail using solutions of Pluronic copolymers [104, 105]. The effect of steady shear, applied using a Couette cell, on the orientation of a fcc structure in $PEO_{127}PPO_{48}PEO_{127}$ (Pluronic F108) was investigated using SAXS, and transitions between different types of shear flows were elucidated [104]. A twinned fcc structure with a high density of stacking faults due to flow of sliding layers was observed to transform into large homogeneous single crystals of either twin, separated on a millimetre lengthscale, upon application of LAOS [105]. The same system has recently been investigated in more detail using SAXS and SANS on samples subjected to steady shear in a Couette cell [106]. Different flow mechanisms were identified, depending on the shear rate. At low shear rates, the fcc structure was locally preserved, and the flow was mediated by defects between crystallites. However, at high shear rates, the melting of the structure was observed through the development of a liquidlike structure factor. Intermediate shear rates ($\dot{\gamma} \approx 50\ s^{-1}$) led to layer sliding, where the close-packed planes slide over one another, aligned parallel to the Couette cell walls.

The application of *in situ* steady shear in a Couette cell enabled the identification, via SANS, of two phases as probable cubic phases in aqueous solutions of the reversed Pluronic copolymer 25R8, with formula $PPO_{15}PEO_{156}PPO_{15}$ (note the hydrophilic midblock) [107]. However, the symmetry of the two distinct cubic phases could not be determined due to the

limited number of reflections observed.

The effect of large-amplitude shearing on cubic phases formed in concentrated aqueous solutions of PEO–PBO diblocks has been investigated in detail using SAXS and SANS [40, 108–12]. In some cases salt was added to change the region of stability of the gel phase. For solutions of $PEO_{40}PBO_{10}$ in 0.2M K_2SO_4, both fcc and bcc phases were identified using SAXS, depending on concentration (in the range 25–40 wt%) and temperature [108]. LAOS was shown to lead to orientation of the hcp layers in the fcc phase, although the effect of shear on the bcc phase was not examined in this work. Changes in the dynamic shear moduli upon application of LAOS to the fcc phase were compared to the global orientation of the system via simultaneous rheology and SAXS experiments (the simultaneous SAXS/rheology instrument is described in detail elsewhere [40]). In subsequent work, the effect of steady shear on the alignment of both bcc and fcc phases was investigated for the same system using SAXS [113]. The bcc gel was found to orient into a polydomain structure, with the close-packed {110} planes both parallel and perpendicular to the shear plane. Two types of fcc phase were observed: one mobile ('soft' gel) and one immobile ('hard' gel). The hard fcc gel could be oriented to form a highly twinned structure, with a significant deviation from the ABCABC... stacking sequence of the ideal structure (figure 13(a)) due to random sequences resulting from slip of {111} hcp planes. The soft gel consisted of a fcc phase with a small grain size, and could not be sheared to form a macroscopically oriented crystal. Shear only homogenized the sample, producing a powder SAXS pattern.

Shear orientation of the bcc phase of $PEO_{90}PBO_{10}$ has been investigated in some detail [109–11]. SAXS with simultaneous rheology was used to determine the alignment of bcc gels following oscillatory shear at different amplitudes and frequencies. Initially {200} planes were found to be normal to the shear direction. However, at higher frequency ($\omega = 100$ rad s^{-1}), LAOS led to a transition to flow with a [111] direction parallel to the shear direction. Flow occurred in {110}, {211} and {321} planes, although flow in {211} planes was dominant [109]. SAXS data showing a sharp increase in alignment of this twinned crystal structure upon increasing strain above a critical amplitude, $\lambda \sim 100\%$ (at a fixed frequency) are shown in figure 18, along with measurements of the dynamic shear moduli, G', G'' which, although not quantitatively meaningful in the nonlinear flow regime, do provide evidence for pronounced shear thinning. At a lower frequency ($\omega = 10$ rad s^{-1}), incomplete alignment of the crystal was observed (in fact pattern 1 in figure 18(b) was obtained following shear at $\lambda = 100\%$, $\omega = 10$ rad s^{-1}). SANS indicated that steady flow in a Couette cell leads to a similar state of alignment to that corresponding to figure 18(b), above a critical shear rate [110]. Thus both strain amplitude and shear rate or frequency control the alignment of the bcc crystal. The mechanism for macroscopic alignment of bcc gels (of $PEO_{90}PBO_{10}$) has been inferred from an investigation of the nonlinear rheology, specifically the shape of the stress waveform accompanying an applied oscillatory strain [111]. This suggested a stick–slip mechanism of flow above a critical shear rate $\dot{\gamma} \approx 50$ s^{-1}. The orientation of a bcc gel formed by $PEO_{210}PBO_{16}$ in water has been probed using SANS, via 'mesoscopic crystallography', where a gel that was aligned using LAOS was probed by rotation with respect to the neutron beam [112]. The SANS patterns that were obtained in different orientations provided information on the three-dimensional structure of the twinned bcc crystal.

Shear-induced orientation of gels of PEO_mPBO_n diblocks with $m \approx 100, 200, 300$ and 400 and $n \approx 18$ proved crucial to the identification of cubic micellar phases, not least because the samples forming a bcc phase only exhibited one order of reflection [114]. Gels were subjected to steady shear in a Couette cell and SAXS was used to determine the shear-induced 'crystal' structure from the angular relationship between the observed Bragg reflections. This enabled results from this series of diblocks to be compiled together with those from earlier studies into a

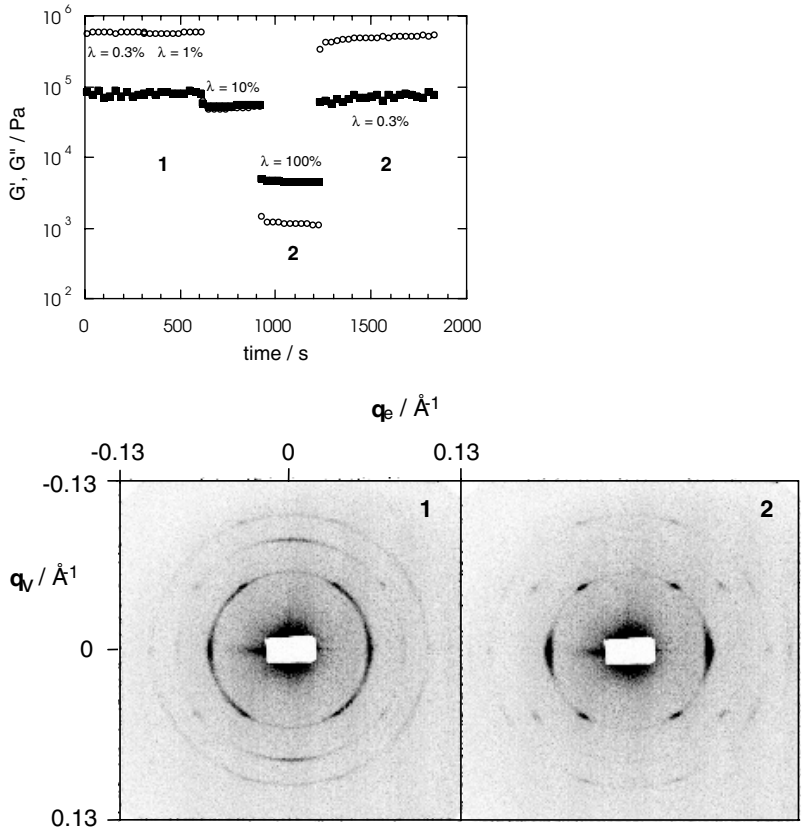

Figure 18. (a) Dynamic shear moduli from simultaneous SAXS/rheology experiments for a 40 wt% gel of $E_{86}B_{10}$ at 25 °C subjected to different strain amplitudes (indicated) at a frequency $\omega = 100$ rad s^{-1}. (b) SAXS patterns obtained concurrently, corresponding to the rheology data as indicated by regime 1 or 2. Macroscopic alignment of the gel was observed for a strain amplitude $\lambda = 100\%$ [109].

'phase diagram' showing regions of stability of fcc and bcc structures as a function of solution concentration and the diblock composition ratio m/n [114]. The effect of shear on an aqueous solution of the diblock $PEO_{55}PBO_8$ forming a fcc structure has been investigated in detail, using SAXS on samples sheared in a Couette cell [115]. Steady shear was found to orient the mesophase into a polydomain structure with the hcp planes both parallel and perpendicular to the shear plane. At low shear rates, a sliding mechanism of flow of hcp layers was identified whereas at higher shear rates, partial melting occurred [115]. SAXS on shear-oriented samples has facilitated the identification of other micellar cubic phases formed in PEO–PBO diblock solutions [116–19].

5. Bicontinuous cubic phases

It is now established that the bicontinuous 'gyroid' (gyr) structure of cubic spacegroup $Ia\bar{3}d$ is an equilibrium phase for AB diblock and ABA triblock copolymers that is stable between the lam and hex phases close to the ODT [120]. The development of this structure from a shear-oriented hex phase was observed to proceed with an epitaxial relationship in the orientation

and spacing of specific lattice planes in the two structures. This was deduced from SANS on a blend of poly(styrene)–poly(2-vinylpyridine) diblock copolymers where the orientation of Bragg peaks in the (v, ∇v) and (v, e) planes in the gyr phase were correlated to those from a shear-oriented hex phase from which the gyr phase developed on heating [120]. The epitaxial relationship between the HPL structure and the gyr phase as well as the hex and gyr phases has also been examined [6, 121]. These transitions appear to be similar to those observed between the lam, hex and gyr phases of lyotropic liquid crystals (where the lam–gyr transition occurs without an intermediate HPL phase) [122, 123]. The slow development of the gyr phase from a shear-oriented HPL phase was investigated via isothermal time-resolved SANS with simultaneous rheology by Vigild and coworkers [6]. It was found that the transition takes as long as 10 h, showing that the HPL phase is highly metastable. The epitaxial relationship deduced from the position and angular distribution of SANS peaks was similar to that reported earlier for the lam–gyr transition in lyotropic liquid crystals [122, 123]. The isothermal growth of the gyroid phase on quenching from a high-temperature shear-oriented hex phase was followed in a similar fashion, and found to occur over a similarly long timescale. However, high-resolution SAXS indicated that rapid quenching led to the formation of the metastable HPL phase which eventually relaxed back into the equilibrium gyr phase. The small-angle scattering patterns from the shear-oriented HPL and gyr phases were also analysed in detail in this paper. It was shown that the gyr phase is a directionally oriented crystal, with a [111] direction along the shear direction that is a zone axis of the slip planes in the crystal [6]. A SAXS pattern from an oriented gyroid phase, together with its indexation, is shown in figure 19. The ten inner reflections arise from the rotation of single crystal domains through an angle θ around the [111] direction, which is the closest packed direction in bcc structures. A full rotation of the reciprocal space runs three times through the sequence of eight patterns in figure 19(b).

The transition from a shear-oriented perpendicular lamellar structure to a gyroid phase in the melt of a PEO–PBO diblock copolymer via an intermediate perforated layer structure has been investigated using SAXS; however, the gyroid phase developed as a polycrystal, without macroscopic orientation [124]. This suggests that the transition does not occur epitaxially, i.e. that gyroid grains nucleate randomly within the metastable perforated layer phase precursor, with a lattice orientation and domain spacing which differs from that of the majority phase. Indeed, the principal wavenumber q^* was shown to vary significantly across the transition [124].

Dair *et al* [125] report that roll-casting of a PS–PI–PS triblock forming an equilibrium gyr phase is not commensurate with maintaining cubic symmetry; it leads instead to a cylindrical structure with rods oriented along the roll-cast direction. However, upon annealing, the gyr phase grows with a [111] direction along the roll-cast direction, as inferred from oriented SAXS patterns.

Crystallization from a gyr phase oriented by oscillatory shear has recently been investigated for a PEO–PBO diblock [126]. Crystallization of poly(ethylene oxide) leads to a semicrystalline lamellar phase under ambient conditions. It was shown that crystallization occurred with a large increase in domain spacing, but that the lamellar orientations were defined by preferred directions in the shear-oriented gyr melt, i.e. crystallographic register was maintained between the two structures, although the transition was not epitaxial due to the change in length scale. In this sense the soft melt phase acted as a template for the hard crystalline phase. In a related work, crystallization from oriented gyr and hex melt phases in an asymmetric poly(ethylene oxide)–poly(isoprene) diblock copolymer was investigated by SAXS [127]. It was found that crystallization from a shear-oriented hex phase led to crystalline lamellar planes parallel to the cylinders, and a step increase in domain spacing.

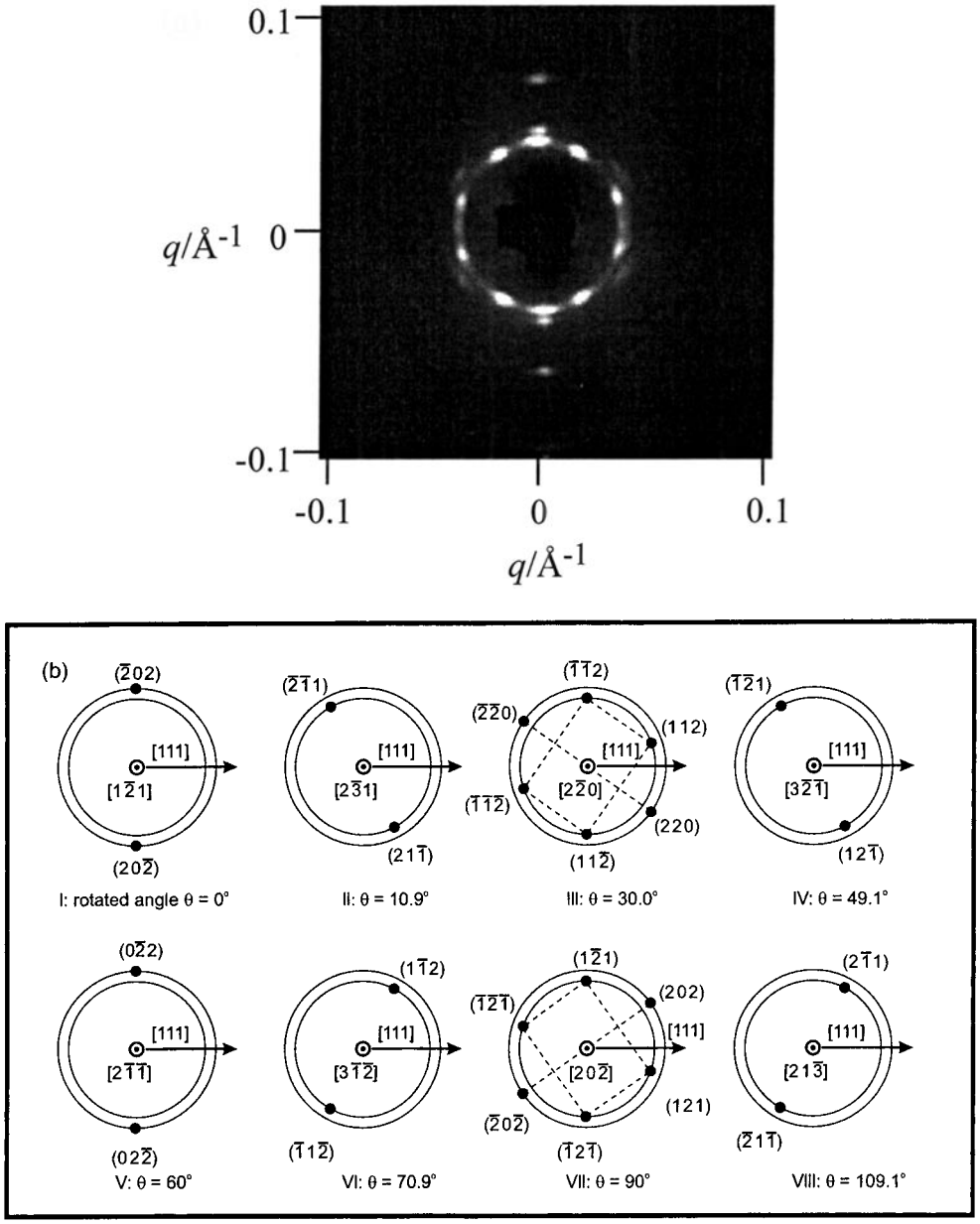

Figure 19. (a) SAXS pattern from the gyr phase of a poly(ethylene-propylene)-poly(dimethylsiloxane) diblock copolymer ($f_{PEP} = 0.67$) oriented using reciprocating shear [6]. (b) Indexation of the first two rings of reflections in the SAXS pattern on the basis of grains rotated around the [111] direction by and angle θ [6].

On heating the oriented crystalline lamellar (lam_c) phase an oriented gyr melt was obtained, which was subjected to shear leading to a change in orientation of the 211-type peaks but not the 220-type peaks, which were arranged hexagonally. The lam_c phase formed by slow crystallization from the gyr melt was characterized by three-fold symmetry of the lamellar

planes, which was ascribed to templating by the hex phase intermediate between the high-temperature gyr phase and the low-temperature lam_c phase. However, the domain spacing increased by 30% on crystallization. These results support the conclusions of Fairclough *et al* [126], i.e. crystallization from the gyroid melt occurs with crystallographic registry between lattice planes but with an increase in domain spacing, although the templating mechanism differs in detail for the two types of copolymer.

6. Summary

The study of the effect of flow on block copolymers is relevant to their processing, as exemplified by the important early work on orientation of block copolymer microstructures induced by extrusion [19, 27, 128]. From a scientific viewpoint, block copolymers serve as model systems for investigating the effect of shear on soft materials because (1) the phase behaviour is now well understood, (2) materials are available in useful quantities and are tractable and (3) experimentally accessible shear rates are comparable to the relaxation rates of the polymeric components. Large-amplitude shear can be used to align lamellar, hexagonal and cubic micellar morphologies, above a critical shear rate (steady shear) or frequency and strain amplitude (oscillatory shear). The lam phase usually aligns with the layer normal along $\nabla \boldsymbol{v}$ (parallel orientation) or along $\boldsymbol{e}$ (perpendicular lamellae), although the transverse orientation (normals along $\boldsymbol{v}$) has been observed as a transient state (and possibly an equilibrium state for multiblock copolymers). Cylinders in the hex phase align along the flow direction, although the orientation of (10) lattice planes can be parallel or perpendicular to the shear plane. The cubic phases exhibit the most complex flow behaviour. A general principle, however, is that a close-packed direction will align with the flow direction, this being a [111] direction for fcc and bcc structures. In the bcc phase, the {110} and/or {211} planes orient parallel to the shear plane. It is not clear why the non-close packed {211} planes should be active flow planes. In the fcc phase, the ABCABC... stacking of hcp layers is disrupted under flow; except at very low shear rates, the layers slide over one another parallel to the shear plane. The gyr phase grows from an oriented hex, lam or HPL phase with a [111] direction parallel to $\boldsymbol{v}$, although in this case flow is in multiple planes which intersect in a common [111] zone axis, corresponding to a directionally oriented crystal.

It is clear that block copolymers will find applications where alignment of self-assembled nanostructures is crucial (in optoelectronics, separation, reinforced composites) and thus an understanding of the coupling between structure and flow behaviour is extremely important.

References

[1] Hamley I W 1998 *The Physics of Block Copolymers* (Oxford: Oxford University Press)
[2] Hajduk D A, Harper P E, Gruner S M, Honeker C C, Kim G, Thomas E and Fetters L J 1994 *Macromolecules* **27** 4063
[3] Förster S, Khandpur A K, Zhao J, Bates F S, Hamley I W, Ryan A J and Bras W 1994 *Macromolecules* **27** 6922
[4] Hamley I W, Koppi K A, Rosedale J H, Bates F S, Almdal K and Mortensen K 1993 *Macromolecules* **26** 5959
[5] Hajduk D A, Takenouchi H, Hillmyer M A, Bates F S, Vigild M E and Almdal K 1997 *Macromolecules* **30** 3788
[6] Vigild M E, Almdal K, Mortensen K, Hamley I W, Fairclough J P A and Ryan A J 1998 *Macromolecules* **31** 5702
[7] Bates F S and Fredrickson G H 1999 *Physics Today* **52** (Feb issue) 32
[8] Ryan A J and Hamley I W 1997 *The Physics of Glassy Polymers* ed R N Haward and R J Young (London: Chapman and Hall)
[9] Drolet F and Fredrickson G H 1999 *Phys. Rev. Lett.* **83** 4317
[10] Bohbot-Raviv Y and Wang Z-G 2000 *Phys. Rev. Lett.* **85** 3428

[11] Helfand E and Sapse A M 1975 *J. Chem. Phys.* **62** 1327
[12] Bates F S and Fredrickson G H 1994 *Macromolecules* **27** 1065
[13] Fredrickson G H and Helfand E 1987 *J. Chem. Phys.* **87** 697
[14] Fredrickson G H and Binder K 1989 *J. Chem. Phys.* **91** 7265
[15] Matsen M W and Schick M 1994 *Phys. Rev. Lett.* **72** 2660
[16] Matsen M W and Bates F S 1996 *Macromolecules* **29** 1091
[17] Hanley K J, Lodge T P and Huang C-I 2000 *Macromolecules* **33** 5918
[18] Keller A, Pedemonte E and Willmouth F M 1970 *Nature* **225** 538
[19] Folkes M J and Keller A 1973 in *The Physics of Glassy Polymer* ed R N Haward (London: Applied Science) p 548
[20] Folkes M J and Keller A 1973 *Block and Graft Copolymers* ed J J Burke and V Weiss (Syracuse: Syracuse University Press) p 87
[21] Fredrickson G H and Bates F S 1996 *Annu. Rev. Mater. Sci.* **26** 501
[22] Honeker C C and Thomas E L 1996 *Chem. Mater.* **8** 1702
[23] Watanabe 1998 *Structures and Properties of Multiphase Polymeric Materials* ed T Araki, Q Tran-Cong and M Shibayama (New York: Dekker) p 317
[24] Hamley I W 2000 *Current Opinion Colloid Interface Sci.* **5** 342
[25] Hamley I W 2001 *Phil. Trans. R. Soc.* **359** 1017
[26] Dlugosz J, Folkes M J and Keller A 1973 *J. Polym. Sci. B: Polym. Phys.* **11** 929
[27] Folkes M J and Keller A 1976 *J. Polym. Sci. B: Polym. Phys.* **14** 833
[28] Wiesner U 1997 *Macromol. Chem. Phys.* **198** 3319
[29] Koppi K A, Tirrell M, Bates F S, Almdal K and Colby R H 1992 *J. Phys. France II* **2** 1941
[30] Zhang U and Wiesner U 1995 *J. Chem. Phys.* **103** 4784
[31] Patel S S, Larson R G, Winey K I and Watanabe H 1995 *Macromolecules* **28** 4313
[32] Riise B L, Fredrickson G H, Larson R G and Pearson D S 1995 *Macromolecules* **28** 7653
[33] Zhang Y, Wiesner U and Spiess H 1995 *Macromolecules* **28** 778
[34] Kannan R M and Kornfield J A 1994 *Macromolecules* **27** 1177
[35] Gupta V K, Krishnamoorti R, Kornfield J A and Smith S D 1995 *Macromolecules* **28** 4464
[36] Okamoto S, Saijo K and Hashimoto T 1994 *Macromolecules* **27** 5547
[37] Polis D L and Winey K I 1996 *Macromolecules* **29** 8180
[38] Polis D L and Winey K I 1998 *Macromolecules* **31** 3617
[39] Pinheiro B S and Winey K I 1998 *Macromolecules* **31** 4447
[40] Hamley I W, Pople J A, Gleeson A J, Komanschek B U and Towns-Andrews E 1998 *J. Appl. Crystallogr.* **31** 881
[41] Polis D L, Smith S D, Terrill N J, Ryan A J, Morse D C and Winey K I 1999 *Macromolecules* **32** 4668
[42] Qiao L and Winey K I 2000 *Macromolecules* **33** 851
[43] Laurer J H, Pinheiro B S, Polis D L and Winey K I 1999 *Macromolecules* **32** 4999
[44] Seguela R and Prud'homme J 1981 *Macromolecules* **14** 197
[45] Cohen Y, Brinkmann M and Thomas E L 2001 *J. Chem. Phys.* **114** 984
[46] Hamley I W, Gehlsen M D, Khandpur A K, Koppi K A, Rosedale J H, Schulz M F, Bates F S, Almdal K and Mortensen K 1994 *J. Phys. France II* **4** 2161
[47] Qi S and Wang Z G 1997 *Phys. Rev.* E **55** 1682
[48] Balsara N P and Hammouda B 1994 *Phys. Rev. Lett.* **72** 360
[49] Balsara N P, Hammouda B, Kesani P K, Jonnalagadda S V and Straty G C 1994 *Macromolecules* **27** 2566
[50] Wang H, Kesani P K, Balsara N P and Hammouda B 1997 *Macromolecules* **30** 982
[51] Pople J A, Hamley I W, Fairclough J P A, Ryan A J, Hill G and Price C 1999 *Polymer* **40** 5709
[52] Vigild M E, Chu C, Sugiyama M, Chaffin K A and Bates F S 2001 *Macromolecules* **34** 951
[53] Mortensen K 1996 *J. Phys.: Condens. Matter* **8** 103
[54] Zipfel J, Lindner P, Tsianou M, Alexandridis P and Richtering W 1999 *Langmuir* **15** 2599
[55] Zipfel J, Berghausen J, Schmidt G, Lindner P, Alexandridis P, Tsianou M and Richtering W 1999 *Phys. Chem., Chem. Phys.* **1** 3905
[56] Richter D, Schneiders D, Monkenbusch M, Willner L, Fetters L J, Huang J S, Lin M, Mortensen K and Farago B 1997 *Macromolecules* **30** 1053
[57] Hadziioannou G, Mathis A and Skoulios A 1979 *Colloid. Polym. Sci.* **257** 15
[58] Hadziioannou G, Mathis A and Skoulios A 1979 *Colloid. Polym. Sci.* **257** 136
[59] Almdal K, Bates F S and Mortensen K 1992 *J. Chem. Phys.* **96** 9122
[60] Morrison F A, Mays J W, Muthukumar M, Nakatani A I and Han C C 1993 *Macromolecules* **26** 5271
[61] Nakatani A I, Morrison F A, Douglas J F, Mays J W, Jackson C L, Muthukumar M and Han C C 1996 *J. Chem.*

Phys. **104** 1589
[62] Winter H H, Scott D B, Gronski W, Okamoto S and Hashimoto T 1993 *Macromolecules* **26** 7236
[63] Tepe T, Schulz M F, Zhao J, Tirrell M, Bates F S, Mortensen K and Almdal K 1995 *Macromolecules* **28** 3008
[64] Bates F S, Koppi K A, Tirrell M, Almdal K and Mortensen K 1994 *Macromolecules* **27** 5934
[65] Sakurai S, Momii T, Taie K, Shibayama M, Nomura S and Hashimoto T 1993 *Macromolecules* **26** 485
[66] Jackson C L, Barnes K A, Morrison F A, Mays J W, Nakatani A I and Han C C 1995 *Macromolecules* **28** 713
[67] Koppi K A, Tirrell M, Bates F S, Almdal K and Mortensen K 1994 *J. Rheol.* **38** 999
[68] Arridge R G C and Folkes M J 1972 *J. Phys. D: Appl. Phys.* **5** 344
[69] Odell J A and Keller A 1977 *Polym. Eng. Sci.* **17** 544
[70] Hadziioannou G, Mathis A and Skoulios A 1979 *Colloid. Polym. Sci.* **257** 337
[71] Tarasov S G, Tsvankin D Y and Godovskii Y K 1979 *Polym. Sci. USSR* **20** 1728
[72] Pakula T, Saijo K, Kawai H and Hashimoto T 1985 *Macromolecules* **18** 1294
[73] Honeker C C, Thomas E L, Albalak R J, Hajduk D A, Gruner S M and Capel M C 2000 *Macromolecules* **33** 9395
[74] Honeker C C and Thomas E L 2000 *Macromolecules* **33** 9407
[75] Fairclough J P A *et al* 2000 *Polymer* **41** 2577
[76] Daniel C, Hamley I W and Mortensen K 2000 *Polymer* **41** 9239
[77] Daniel C and Hamley I W 2000 *Rheol. Acta* **39** 191
[78] Balsara N P, Dai H J, Kesani P K, Garetz B A and Hammouda B 1994 *Macromolecules* **27** 7406
[79] Balsara N P and Dai H J 1996 *J. Chem. Phys.* **105** 2942
[80] Pople J A, Hamley I W, Fairclough J P A, Ryan A J and Booth C 1998 *Macromolecules* **31** 2952
[81] Pople J A, Hamley I W, Terrill N J, Fairclough J P A, Ryan A J, Yu G-E and Booth C 1998 *Polymer* **39** 4891
[82] Okamoto S, Saijo K and Hashimoto T 1994 *Macromolecules* **27** 3753
[83] Almdal K, Koppi K and Bates F S 1993 *Macromolecules* **26** 4058
[84] Shin G, Sakamoto N, Saijo K, Suehiro S, Hashimoto T, Ito K and Amemiya Y 2000 *Macromolecules* **33** 9002
[85] Inoue T, Moritani M, Hashimoto T and Kawai H 1971 *Macromolecules* **4** 500
[86] Richards R W and Welsh G 1995 *Eur. Polym. J.* **31** 1197
[87] Prasman E and Thomas E L 1998 *J. Polym. Sci. B: Polym. Phys.* **36** 1625
[88] Higgins J S, Blake S, Tomlins P E, Ross-Murphy S B, Staples E, Penfold J and Dawkins J V 1988 *Polymer* **29** 1968
[89] Phoon C L, Higgins J S, Allegra G, van Leeuwen P and Staples E 1993 *Proc. R. Soc.* A **442** 221
[90] McConnell G A, Lin M Y and Gast A P 1995 *Macromolecules* **28** 6754
[91] Loose W and Ackerson B J 1994 *J. Chem. Phys.* **101** 7211
[92] McConnell G A and Gast A P 1997 *Macromolecules* **30** 435
[93] Kleppinger R, Mischenko N, Theunissen E, Reynaers H L, Koch M H J, Almdal K and Mortensen K 1997 *Macromolecules* **30** 7012
[94] Reynders K, Mischenko N, Mortensen K, Overbergh N and Reynaers H 1995 *Macromolecules* **28** 8699
[95] Mischenko N, Reynders K, Mortensen K, Overberg N and Reynaers H 1996 *J. Polym. Sci. B: Polym. Phys.* **34** 2739
[96] Mortensen K 1992 *Europhys. Lett.* **19** 599
[97] Mortensen K, Brown W and Nordén B 1992 *Phys. Rev. Lett.* **68** 2340
[98] Mortensen K 1993 *Prog. Colloid. Polym. Sci.* **91** 69
[99] Eiser E, Molino F, Porte G and Diat O 2000 *Phys. Rev.* E **61** 6759
[100] Ackerson B J and Clark N A 1984 *Phys. Rev.* A **30** 906
[101] Eiser E, Molino F and Porte G 2000 *Eur. Phys. J.* E **2** 39
[102] Daniel C, Hamley I W, Wilhelm M and Mingvanish W 2001 *Rheol. Acta* **40** 39
[103] Holmqvist P, Daniel C, Hamley I, Mingvanish W and Booth C 2001 *Colloids Surfaces* A at press
[104] Berret J-F, Molino F, Porte G, Diat O and Lindner P 1996 *J. Phys.: Condens. Matter* **8** 9513
[105] Diat O, Porte G and Berret J-F 1996 *Phys. Rev.* B **54** 14 869
[106] Molino F R, Berret J-F, Porte G, Diat O and Lindner P 1998 *Eur. Phys. J.* B **3** 59
[107] Mortensen K 1997 *Macromolecules* **30** 503
[108] Pople J A, Hamley I W, Fairclough J P A, Ryan A J, Komanschek B U, Gleeson A J, Yu G-E and Booth C 1997 *Macromolecules* **30** 5721
[109] Hamley I W, Pople J A, Fairclough J P A, Ryan A J, Booth C and Yang Y-W 1998 *Macromolecules* **31** 3906
[110] Hamley I W, Pople J A, Booth C, Yang Y-W and King S M 1998 *Langmuir* **14** 3182
[111] Hamley I W, Pople J A, Booth C, Derici L, Impéror-Clerc M and Davidson P 1998 *Phys. Rev.* E **58** 7620
[112] Hamley I W, Mortensen K, Yu G-E and Booth C 1998 *Macromolecules* **31** 6958
[113] Hamley I W *et al* 1998 *J. Chem. Phys.* **108** 6929

[114] Hamley I W, Daniel C, Mingvanish W, Mai S-M, Booth C, Messe L and Ryan A J 2000 *Langmuir* **16** 2508
[115] Daniel C, Hamley I W, Mingvanish W and Booth C 2000 *Macromolecules* **33** 2163
[116] Hamley I W, Pople J A, Ameri M, Attwood D, Booth C and Ryan A J 1998 *Macromol. Chem. Phys.* **199** 1753
[117] Kelarakis A, Havredaki V, Derici L, Yu G-E, Booth C and Hamley I W 1998 *J. Chem. Soc. Faraday Trans.* **94** 3639
[118] Derici L, Ledger S, Mai S-M, Booth C, Hamley I W and Pedersen J S 1999 *Phys. Chem., Chem. Phys.* **1** 2773
[119] Kelarakis A, Mingvanish W, Daniel C, Li H, Havredaki V, Booth C, Hamley I W and Ryan A J 2000 *Phys. Chem., Chem. Phys.* **2** 2755
[120] Schulz M F, Bates F S, Almdal K and Mortensen K 1994 *Phys. Rev. Lett.* **73** 86
[121] Zhao J, Majumdar B, Schulz M F, Bates F S, Almdal K, Mortensen K, Hajduk D A and Gruner S M 1996 *Macromolecules* **29** 1204
[122] Ranǫn Y and Charvolin J 1988 *J. Phys. C: Solid State Phys.* **92** 2646
[123] Clerc M, Levelut A M and Sadoc J F 1991 *J. Phys. France II* **1** 1263
[124] Hamley I W, Fairclough J P A, Ryan A J, Mai S-M and Booth C 1999 *Phys. Chem., Chem. Phys.* **1** 2097
[125] Dair B J, Avgeropoulos A, Hadjichristidis N, Capel M and Thomas E L 2000 *Polymer* **41** 6231
[126] Fairclough J P A *et al* 2001 *J. Chem. Phys.* **114** 5425
[127] Hamley I W and Floudas G 2001 in preparation
[128] Dlugosz J, Keller A and Pedemonte E 1970 *Kolloid ZuZ Polymere* **242** 1125
[129] Maring D and Wiesner U 1997 *Macromolecules* **30** 660
[130] Gupta V K, Krishnamoorti R, Kornfield J A and Smith S D 1996 *Macromolecules* **29** 1359